University of Windsor
Scholarship at UWindsor

Electronic Theses and Dissertations | Theses, Dissertations, and Major Papers

5-2021

Underwater Pipeline Leakage Detection Using Vision Based Techniques: Semi-AUV (SAUV) Approach

anisha Alkarim Thobhani
University of Windsor

Follow this and additional works at: https://scholar.uwindsor.ca/etd

Part of the Electrical and Computer Engineering Commons

Recommended Citation

Thobhani, anisha Alkarim, "Underwater Pipeline Leakage Detection Using Vision Based Techniques: Semi-AUV (SAUV) Approach" (2021). *Electronic Theses and Dissertations*. 8834.
https://scholar.uwindsor.ca/etd/8834

This online database contains the full-text of PhD dissertations and Masters' theses of University of Windsor students from 1954 forward. These documents are made available for personal study and research purposes only, in accordance with the Canadian Copyright Act and the Creative Commons license—CC BY-NC-ND (Attribution, Non-Commercial, No Derivative Works). Under this license, works must always be attributed to the copyright holder (original author), cannot be used for any commercial purposes, and may not be altered. Any other use would require the permission of the copyright holder. Students may inquire about withdrawing their dissertation and/or thesis from this database. For additional inquiries, please contact the repository administrator via email (scholarship@uwindsor.ca) or by telephone at 519-253-3000ext. 3208.

Underwater Pipeline Leakage Detection Using Vision Based Techniques: Semi-AUV(SAUV) Approach

By

Manisha Alkarim Thobhani

A Thesis
Submitted to the Faculty of Graduate Studies through
the Department of Electrical and Computer Engineering
in Partial Fulfillment of the Requirements for
the Degree of Master of Applied Science at the
University of Windsor

Windsor, Ontario, Canada

© 2021 Manisha Thobhani

Underwater Pipeline Leakage Detection Using Vision Based Techniques: Semi-AUV(SAUV) Approach

By

Manisha Alkarim Thobhani

APPROVED BY:

_____

J. Ahamed
Department of Mechanical, Automotive and Materials Engineering

_____

E. Abdel-Raheem
Department of Electrical & Computer Engineering

_____

M. Saif, Co-Advisor
Department of Electrical & Computer Engineering

_____

S. Alirezaee, Co-Advisor
Department of Electrical & Computer Engineering

May 17, 2021

DECLARATION OF ORIGINALITY

I hereby certify that I am the sole author of this thesis and that no part of this thesis has been published or submitted for publication.

I certify that, to the best of my knowledge, my thesis does not infringe upon anyone's copyright nor violate any proprietary rights and that any ideas, techniques, quotations, or any other material from the work of other people included in my thesis, published or otherwise, are fully acknowledged in accordance with the standard referencing practices. Furthermore, to the extent that I have included copyrighted material that surpasses the bounds of fair dealing within the meaning of the Canada Copyright Act, I certify that I have obtained a written permission from the copyright owner(s) to include such material(s) in my thesis and have included copies of such copyright clearances to my appendix.

I declare that this is a true copy of my thesis, including any final revisions, as approved by my thesis committee and the Graduate Studies office, and that this thesis has not been submitted for a higher degree to any other University or Institution.

ABSTRACT

This thesis intends to convert a Remote Operated Vehicle (ROV) to a Semi-Autonomous Underwater Vehicle (SAUV) using a vision-based control system. The SAUV was used for automatic underwater gas pipeline tracking and leakage detection. the leakages in the pipeline using Computer Vision. The SAUV was designed to operate both manually and automatically in underwater conditions. The proposed SAUV has 6 thrusters to achieve 4 degrees of freedom controlled by the controller unit and powered by LiPo battery packs. Our underwater vehicle is equipped with sensors providing continuous feedback signals to automatically control the vehicle to track predefined trajectories. The SAUV can be self-stabilized as the center of gravity and center of buoyancy of the vehicle is positioned in such a way in the predefined plan.

The SAUV captures images to perform line tracking along with the pipeline and gas bubble images during its mission. The multi-core umbilical cable is used here for the video signal, the feedback signal, and battery charging lines. This will be used only for development and test purposes and will be removed during autonomous missions. For performing all operations, various control schemes such as computer vision algorithm for object detection using python programming, OpenCV, Hough Transform Theory, etc. are applied.

The proposed SAUV is expected to pave the way for the development of advanced underwater oil and gas pipeline industrial applications by ocean scientists.

Keywords: *Semi-Autonomous Underwater Vehicle (SAUV), SAUV Balancing; Vision-based Tracking; Vision-based blob detection*

DEDICATION

To my husband and son, for their continuous support

To my supervisor, for his continuous help and guidance

ACKNOWLEDGMENTS

I would love to express my great appreciation to my advisor Dr Mehrdad Saif and co-advisor Dr. Shahpour Alirezaee for their continuous guidance and support during this journey. This thesis would not have been at this knowledge and quality levels without his sincere effort and time. His support was not only limited to supervising and recommending research topics; he always encourages his graduate students to never give up, think critically and outside the box. One of the most challenging experiences during this journey was selecting a research topic, but with the help of Dr. Shahpour Alirezaee, we overcame this obstacle and succeeded.

I would like to express my gratitude to all my committee members for their valuable feedback.

Finally, I would like to thank my family for their endless love and support.

TABLE OF CONTENTS

DECLARATION OF ORIGINALITY iii

ABSTRACT iv

DEDICATION v

ACKNOWLEDGEMENT vi

LIST OF TABLES x

LIST OF FIGURES xi

CHAPTER 1 INTRODUCTION 1

1.1 Research Motivation 1

1.2 Problem Statement 1

1.3 Objectives 3

1.4 Scope of Research 3

1.5 Thesis Structure 4

CHAPTER 2 STATE OF THE ART 6

2.1 Overview 6

2.2 Literature Review 6

2.3 Existing Methods for Leakage Detection 7

2.3.1 Exterior Methods 9

2.3.2 Interior Methods 11

2.3.3 Visual Methods 13

2.4 Performance Comparison of Leakage Detection Methods 15

2.5 Research Gap and Open Issues 16

2.6 Conclusion 19

CHAPTER 3 PROPOSED APPROACH: THEORETICAL BACKGROUND 20

3.1 Overview 20

3.2 Advanced Computer Vision-based Technology 22

3.2.1 Image Processing 25

3.2.2 Image Preprocessing for underwater object detection 26

3.2.3 Canny Edge Detection 27

3.2.4 Hough Transform 31

3.3 Conclusion 35

CHAPTER 4 PROPOSED APPROACH: SAUV VISION-BASED SYSTEM 36

4.1 SAUV Concept 36

4.1.1 Architecture 36

4.1.2 System Components 39

4.1.3 Vision-based Tracking 50

4.1.4 Vision-based blob(leakage)Detection 53

4.1.5 SAUV Balancing 54

4.2 Conclusion 56

CHAPTER 5 DEVELOPMENT AND TEST RESULTS 57

5.1 Overview 57

5.2 SAUV performance in Manual/Auto mode 57

5.3 SAUV Balancing 59

5.3.1 Influence of turbulence of water in balancing 63

5.4 Vision-based SAUV Tracking 64

5.4.1 Influence of Turbulence on SAUV Line Tracking 67

5.4.2 Influence of Lighting Conditions on SAUV 69

5.4.3 Influence of Irregular Line on SAUV Line Tracking 71

5.5 Vision-based spillage Detection by SAUV 74

5.5.1 Influence of Blob Size in Spillage Detection 75

5.5.2 Blob (Spillage) Detection Accuracy 78

5.6 Challenges and Limitations 80

5.7 Conclusion 81

CHAPTER 6 CONCLUSION 82

6.1 Discussion 82

6.2 Significance 83

6.3 Future Work 83

REFERENCES 84

VITA AUCTORIS 88

LIST OF TABLES

Table1: Performance Comparison of Pipeline leakage detection methods 15

Table 2: Drifting Deviation and RMSE on static position of MPU 6050 sensor 62

Table 3: Drifting Deviation and RMSE on movement position of MPU 6050 sensor..... 62

Table 4: Recorded Results of Area in pixels for Blob Detection Experiment..... 77

LIST OF FIGURES

Fig. 1: Pi- chart of Statics of the sources of the pipeline failure 2

Fig. 2: Flowchart of pipeline leakage detection Systems 8

Fig. 3: Exterior Method - Vapor Sampling 10

Fig. 4: Interior Method – Negative pressure wave 11

Fig. 5: Visual Method – Underwater Vehicle 14

Fig. 6: Sharing concepts of Computer Vision System 24

Fig. 7: Object detection block diagram 25

Fig. 8: Image processing of pipeline edge detection 27

Fig. 9 & Fig. 10: Non – Maximum Suppression Example 29

Fig. 11: Line Representation in X-Y plane 32

Fig. 12: The domain (m, c) 32

Fig. 13 and 14: The plotting of points P1, P2 on the (m, c) plane 33

Fig. 15: Input Image – After edge detection 35

Fig. 16 Image after Voting (Dembele, n.d.) 35

Fig. 17 Block diagram of proposed SAUV approach 37

Fig. 18 Arrangement of DC Motors 38

Fig. 19 Brushless DC Motors 39

Fig. 20 Bi-directional Control through ESC and controller 41

Fig. 21 LiPo Battery for used in SAUV 43

Fig. 22 Pi Camera (NoIR V2) 44

Fig. 23a Raspberry Pi-GPIO 45

Fig. 23b Raspberry Pi-GPIO– Model B 46

Fig. 24 MPU 6050 with controller 48

Fig. 25 MPU – 6050 Orientation and Polarity Rotation 48

Fig. 26 Accelerometer motion in 3- Axis 49

Fig. 27 Vision- based tracking 51

Fig. 28 Centroid of Contour area Cx 52

Fig. 29 Vision-based blob detection 53

Fig. 30 SAUV balancing 55

Fig. 31 Experimental Set-up of Auto/Manual Mode: SAUV 58

Fig. 32 Experimental Set-up of SAUV balancing 59

Fig. 33 MPU6050 with Motors E1 and E2 60

Fig. 34 MPU6050 with Motors E3 and E4 60

Fig. 35 MPU6050 with Motors E1, E2, E3 and E4 Motors 61

Fig. 36 Tilted position and steady position of MPU6050 with ESC DC Motor 62

Fig. 37 Thrust Measurement during experiment 63

Fig. 38 Analysis of SAUV Balancing in -90 to +90 degrees 64

Fig. 39 Arrangement of motors for Line Tacking..... 65

Fig. 40 Test results for Line Tracking..... 66

Fig. 41 Graphical Representation of Test results for Line Tracking..... 67

Fig. 42 Test result of Line tracking with Turbulence 68

Fig. 43 Graphical Representation of Test results for Line Tracking with Turbulence 68

Fig. 44 Test Result with Low Lighting..... 69

Fig. 45 Test result of Line Tracking in the Dark with Add-On Lighting 70

Fig. 46 Graphical Representation of Line Tracking in Dark with Add-On Lighting..... 70

Fig. 47 Test result of Line Tracking in the Dark with Add-On Lighting and Turbulence 71

Fig. 48 Test result of Irregular Line Tracking 72

Fig. 49 Test result of Irregular Line Tracking with Turbulence 72

Fig. 50 Graphical representation of Irregular Line Tracking without Filter..... 73

Fig. 51 Graphical representation of Irregular Line Tracking with Filter..... 73

Fig. 52 Experimental Set-up for blob detection 74

Fig. 53 Test Result of Blob Detection..... 75

Fig. 54 Influence of blob sizes in spillage detection 76

Fig. 55 Graphical Representation of influence of blob sizes in spillage detection..... 76

Fig. 56 Graphical Representation of Blob Detection Comparison in Normal Operation..... 78

Fig. 57 Graphical Representation of Blob Detection Accuracy in Normal Operation..... 79

Fig. 58 Graphical Representation of Blob Detection Accuracy In Turbulence 79

Fig. 59 Before (Left) and After (Right) Arrangement of DC Motors for SAUV Balancing..... 80

CHAPTER 1

INTRODUCTION

1.1 Research Motivation

Nowadays, Underwater research has been becoming a more interesting subject for scientists and entrepreneurs. It is essential in various applications such as undersea environment movement, safety, rescue, oceanographic surveys, natural disaster warning system, and industrial applications. One of the most practical applications of underwater vehicles is underwater oil and gas submarine pipeline network exploration. In fact, the submarine pipeline is a major platform in conveying fossil fuels, gases, chemicals, and other essential hydrocarbon fluids. In addition, it is a major driving force to run the economy of many countries including Canada. Moreover, it is a reliable and economical source for transporting petroleum products. The submarine pipeline network is designed in such a way that they can sustain in severe underwater environmental conditions and also distribute the oil or gas production to the distribution depot [1].

1.2 Problem Statement

As transportation of petroleum fluid has become more popular through submarine pipelines across the whole world in recent decades, there is a possibility of major and critical accidents due to leakages in submarine pipelines. The pipeline failure can bring about major irreversible damages including human fatality, economical disasters, financial losses, and extreme environmental pollution. The major causes of pipeline leakages are device/material

failure, joint problems, or corrosion. Therefore, it is of paramount importance to find out leakages as soon as possible to avert the aforementioned catastrophes. Prompt leakage detection is also essential for avoiding delay in operation and schedule the dependent operation. It is noticeable that maintenance operations are scheduled in consideration of underwater weather conditions which are unpredictable, so swift leakage detection is essential to schedule the operation in a safe and timely manner. About 50% of submarine pipelines are aged and vulnerable, increasing the chances of pipeline failures due to pipeline corrosion.

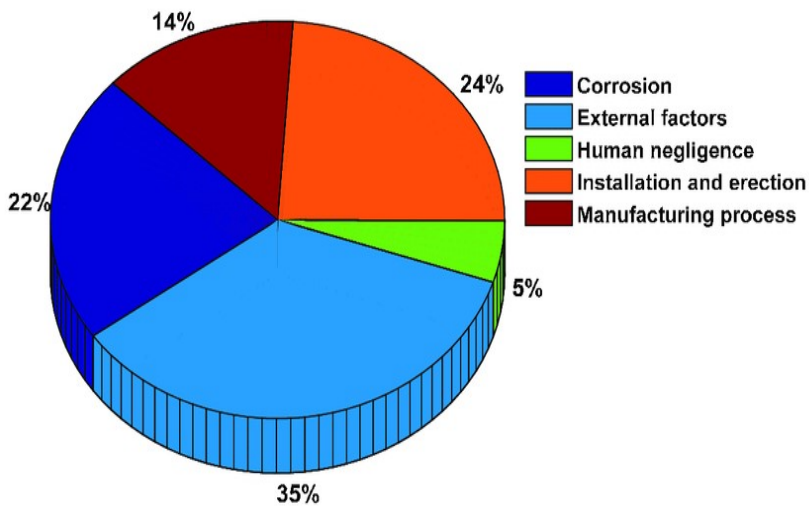

Fig. 1: Pi- chart of Statics of the sources of the pipeline failure [20]

Fig. 1 shows the important factors including corrosion, human negligence, installation and erection damages, manufacturing process damages of the pipeline spillage detection. According to statics, most of the leakages are occurred due to corrosion and underwater weather conditions. However, the impact of these factors can be minimized with prompt and accurate detection of spillage. Though several pipeline leakage detection methods have been

proposed during the last decades, there is still more room for improvement to develop more effective, economical, reliable, and prompt leakage detection methods.

1.3 Objectives

The overriding aim of this thesis is to develop a methodology that can detect the leakages of the pipeline promptly and effectively without human intervention i.e., autonomously. To do so, advanced equipment and technologies such as vision sensors, controllers, and also computer vision have been leveraged to make the SAUV operation smooth and prompt.

The research thesis statement of this research could be formulated as follows:

A Semi-Autonomous Underwater Vehicle based on a vision system will be developed to detect submarine pipeline leakages. It would provide an effective and prompt solution to avoiding major ecological, environmental and human fatalities. It would include advanced gadgets and technologies such as sensors, cameras, control engineering, machine learning, and computer vision.

1.4 Scope of Research

This research proposal can be applied to submarine oil and gas pipeline industries which is a great economic booster for many countries nowadays. Also, it can be applied to many others projects such as underwater target detection and classification in areas where humans can not access easily. Moreover, this fundamental principle can be useful in oceanographic research and surveys. The use of this application is limited to some underwater applications such as disaster warning systems, rescue, military surveillance.

1.5 Thesis Structure

The thesis is presented in 5 chapters in which Chapter2 summarizes the available literature review on submarine pipeline leakage detection and topics related to this research. Chapter 3 describes a new methodology based on computer vision systems including design, architecture, and control programming. Chapter 4 shows the results and presents discussions on the experimental case scenarios. Chapter 5 provides a conclusion, a discussion of the novelty of the presented research, and suggestions for future work.

CHAPTER 2

STATE OF THE ART

2.1 Overview

In this chapter, previous work addressing the submarine pipeline leakage detection methodologies, para-methods, and their different evaluation and comparison in challenging underwater environments are reviewed. As spillage detection of the gas submarine pipelines is an essential task to prevent environmental and economical losses due to the pipeline leakages, several methods have existed to serve this purpose. However, each method has its benefits and limitations for the underwater environment, the research of finding new methods has been continued for recent decades. Here, all existing methods and sub-methods are discussed and reviewed with different perspectives. At the end of this chapter, research gaps and open issues are discussed.

2.2 Literature Review

In recent decades, to leverage the submarine pipeline leakage detection several methods have been introduced or advanced for better performance and overcome limitations of previous methods. The leak detection methods must be sensitive, reliable, accurate, and robust regardless regulations of the nation [3]. However, the spillage detection task for the submarine pipelines is very expensive in terms of deployment of equipment and operations [20]. Also, the underwater weather conditions are challenging in terms of temperature,

transparency, and wireless communication. In the underwater environment, the sensors receive the signal significantly and distort very easily [24].

Depending on the degree of automation, detection methods can be classified into automatic detection, semi-automatic detection, and manual detection [24]. The detection technology has been divided into direct detection and indirect detection as per the intuitive level of the detection data [29]. Additionally, according to some scholars, the spillage detection methods are divided into optical methods and non – optical methods [8]. As per the most recent classification, the detection methods are divided into hardware-based methods and software–based methods [31]. To classify the existing methods technically, they are grouped into three categories: internal or computational, external and visual or biological [20]. Additionally, the internal approach includes software-based methods that use smart computational algorithms through sensor monitoring of the internal movement of the pipeline. Remote monitoring is being done by the camera and sensing system designated through smart dogs, smart pigs, and Autonomous Underwater Vehicle [20].

According to this classification of the pipeline leakage detection techniques, we discuss here some methods that include various key concepts of the technology. A Lidar System (Hardware-based method) works on the principle of spectral absorption, light is absorbed by gas molecules and concentrated gas is gained after analyzing the laser's initial power and echo power [2]. Same as earlier, in the sound wave method, the key concept is to determine the wave velocity of the sound wave [17]. For the Acoustic emission method, the installed sound sensor receives the noise generated by the pipeline leaks and it passes through the analysis of the full waveform and locates the leakage point [26]. This emission technology is

highly sensitive among all the methods and it performs accurate localization [5]. Accelerometers, Signal processing, A Software-based method refers to the method of aggregating signals from multiple stations to generate a mass flow balanced image changes according to internal movement of the pipeline [6]. In a Neural Network Method, the artificial neural network has been used with a construction of a neurons' input matrix of leakage characteristics to identify the leakage signal as it can simulate any continuous nonlinear function and learn from the data [32]. In addition, the adaptive neural network does not need any training data from the actual leakage for the training itself, but it can learn from online fault and adaptable in a dynamic background noise environment [21].

2.3 Existing Methods for Leakage Detection

The pipeline leakage detection methods have been introduced with different working principles and approaches. The existing methods available for pipeline leakage detection are acoustic emission, fiber optic sensor, ground penetration radar, negative pressure wave, pressure point analysis, dynamic modeling, vapor sampling, infrared thermography, digital signal processing, mass-volume balance. They are classified by some authors into two categories: hardware and software-based methods. For the technical perspective and further research, they are classified into main three groups: 1. Internal methods, 2. External methods and 3. Visual/ Biological methods [20]. For exterior methods, different types of sensing systems are utilized outside the submarine pipeline network to detect the leakages. On the other way, the leakage detection can be done through the measurement of internal

movement of the internal fluid of the pipeline through the application of software-based computational algorithms in the internal methods.

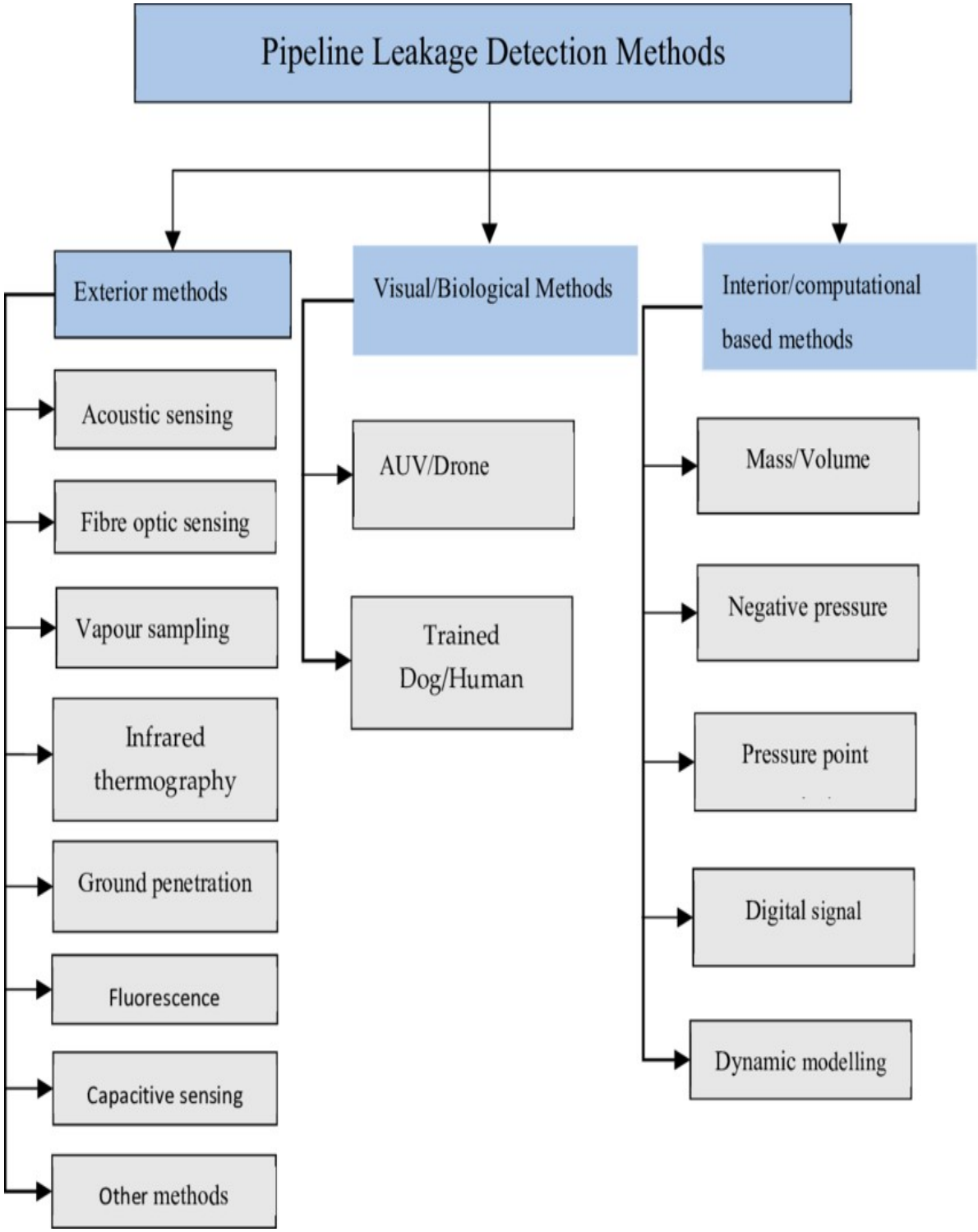

Fig. 2: Flowchart of pipeline leakage detection Systems [20]

In addition, the third method includes a biological or visual detection by a trained dog, and underwater Vehicle is very popular nowadays. In many countries, the Government has set up rules for the deployment of the leakage detection system to ensure the safety of the pipelines, in which leakage system must be sensible, reliable, accurate, and robust [3]. However, research has been ongoing for so many years, to make the pipeline leakage system suitable to fulfill safety requirements and underwater weather conditions. In Fig. 2, the flow chart has been shown to the detailed classification of the pipeline leakage detection systems.

2.3.1 Exterior Methods

Exterior methods mainly include the utilization of the sensing devices that monitor the external part of the pipeline. In these methods, abnormalities and leakages surrounding the pipeline are detected. Although sub-methods are working on different principles, the sensing devices need infrastructure to make physical contact between the sensor probes and the pipeline. The sensing devices include acoustic sensing, fiber optic sensing, vapor sampling, infrared thermography, and ground penetration radar. The one example of the external method has been discussed below.

As shown in Fig. 3, Vapor Sampling Method is one of the methods which work on the principle of determining the level or amount of hydrocarbon vapor inside the pipeline to detect spillage from the pipeline. The gas tube mounted outside the submarine pipeline is filled with air at the atmospheric level and it is pressure dependent. Oil or gas leaking which results in gas bubbles or gas concentration is a function of pumping time. While pipeline leakage occurs, it creates vapor or gas diffuses into the gas tube and after a certain time, it

generates a signal as an indication of hydrocarbon flit in the tube. As the gas concentration is proportional to the leak peak, as gas concentration increases, leak peak increases.

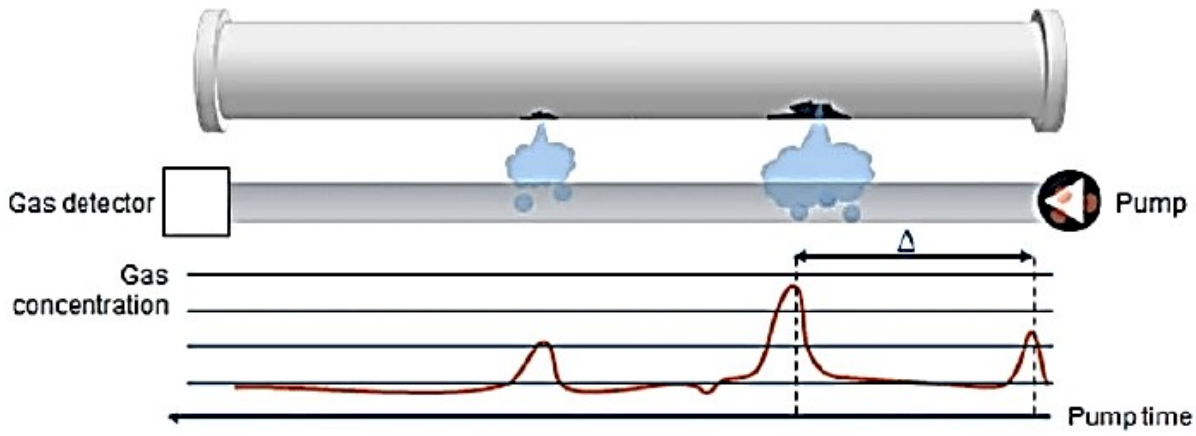

Fig. 3: Exterior Method - Vapor Sampling [3]

Moreover, there are different types of vapor-sampling-based pipeline leakage detection methods existing as per pipeline sizes and underwater environment. The sniffer tubes were for detecting spillage around the pipeline were introduced later. According to the study, a sensor hose is required to be placed underneath the pipeline for prompt detection of the diffusion of the gas outside of the pipeline.

The vapor sampling system has advantages such as small leakage detection, function independently of the pressure of the underwater, super performance in multiphase flow applications. The limitation of this method is that it takes several hours of a long time to respond to the spillage detection.

In this way, exterior methods including Acoustic emission, Fiber Optics Sensing, Vapor Sampling, Infrared Thermography, Ground Penetration Radar, Fluorescence, Electromechanical Impedance, Capacitive Sensing, Spectral Scanners, Lidar Systems,

Electromagnetic reflection have different types of sensing devices to detect pipeline spillage. According to the employment and material they vary in functionality as a medium to high leakage detection, coverage, response time, and execution cost.

2.3.2 Interior Methods

Interior methods mainly use the internal fluid measurement instruments to supervise parameters related to fluid flow in the pipelines. The internal measurement continuously monitors the internal fluid parameters such as pressure, flow, rate, temperature, volume, and other parameters which provides the quantitative information of the petroleum products. The discrepancy between the two pipeline sections is being used to determine the spillage in the pipeline. Interior methods include mass-volume balance, negative pressure waves, pressure point analysis, digital signal processing, and dynamic modeling.

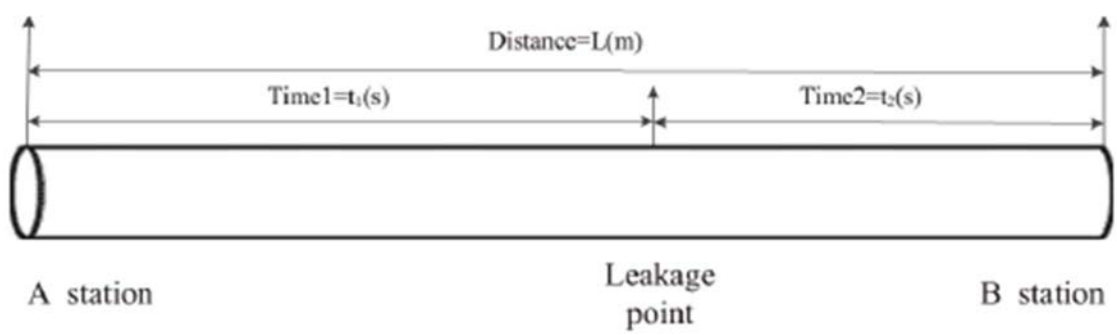

Fig. 4: Interior Method – Negative pressure wave

As shown in Fig. 4, the Negative pressure wave (NPW) method is based on the principle that instantaneous pressure drops and speed variation in the pipeline fluid are caused by a leakage in the pipeline. When a pressure drop occurs, it creates a negative pressure wave at

the leak position. This negative pressure wave propagates the wave through the upstream and downstream ends of the pipeline. The analysis of the wave in terms of the time difference of its ending to the pipeline. There have been developed several techniques developed for signal analysis through a machine learning approach. The localization of leakage point can be calculated through time difference as per below:

$$a = \sqrt{\frac{k/\rho}{1+(k/E)(D/e)C}} \quad \text{.....(1)}$$

where ρ = liquid density in kg/m3

k = liquid bulk modulus of elasticity in Pa

E = modulus of elasticity in Pa

C = correction factor related to the pipeline constraints

e = pipeline thickness in m

The negative Pressure Wave method has advantageous in spillage pipeline detection because it responds fast and it has been able to localize the spillage position adequately and cost-effectively. However, it is only effective in big leakages and gives a false alarm as it gets difficulty in recognizing the normal pressure wave and leakages. There have been some signal processing methods and research is continuing to alleviate these challenges or problems now. For example, morphological filters are employed to reduce the background noise and to achieve the proper geometry of the wave signal.

In this way, interior methods respond variously in terms of fast response, leak size, computational time, underwater environment, leak localization, noise, cost-effectiveness, etc. they have been used as per the priority of the task in the pipeline.

2.3.3 Visual Methods

Visual methods are referred to perform oil spillage detection visually with the utilization of traditional approaches such as trained dogs, experienced personnel, pigs, and underwater vehicles (drones). In this method, trained personnel include humans, pigs, and smart dogs walk along with the pipeline the leakage unusual conditions of the pipeline through visual inspection and smelling the odor coming out from the spills. The pigs are sometimes equipped with sensing and data recording devices to retain sensitive and more accurate information related to spillage of the submarine pipeline. Smart dogs are very sensitive to smelling odor but they can only walk 30-120 min along with the pipeline. In this way, trained personnel are only utilized in onshore and shallow pipeline networks.

As shown in Fig. 5, Remote Operated Vehicle (ROV) is the recent approach of a visual-based method that has emerged the operation of the offshore oil pipeline networks. It is working on the operating principle of the Master-Slave system. ROV is the slave which is operated in harsh conditions of the underwater environment by the human operator who is the master of the system and located in a safe place to control the ROV through joysticks and other input devices. The umbilical cable is utilized here for sending commands and power to the ROV and receiving feedback from it.

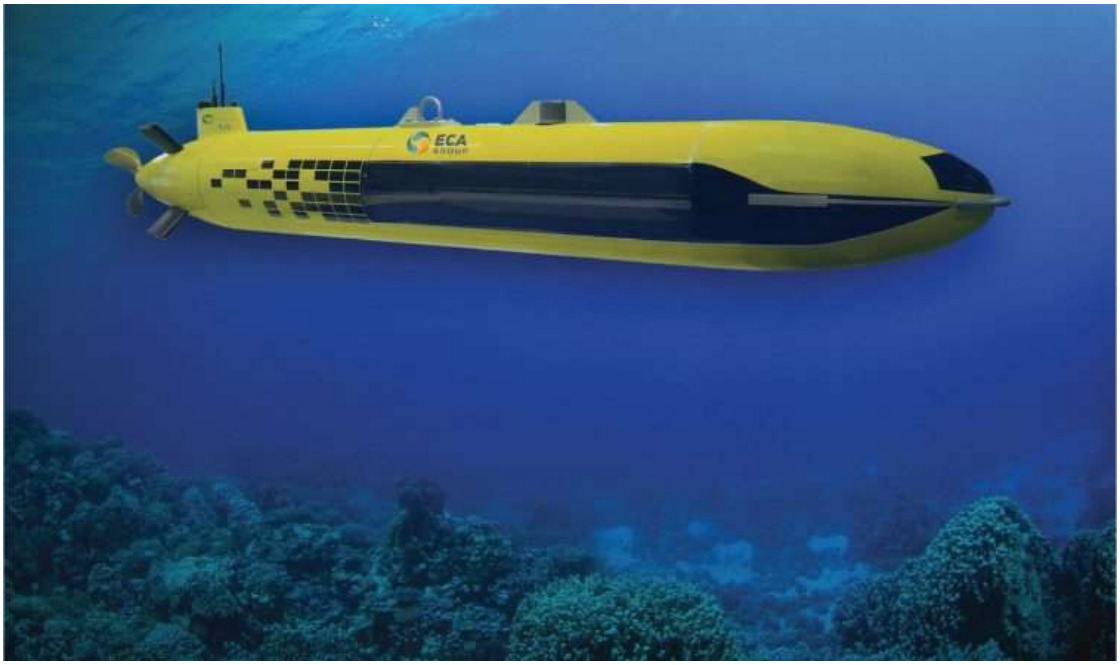

Fig. 5: Visual Method – Underwater Vehicle

ROVs are sustainable and durable for the functioning of spillage detection in the underwater environment area where normally any trained personnel cannot access. The use of the ROV avoids the human causalities caused by the oil or gas spillage in the submarine pipelines. However, ROVs are operated with minimal human intervention, but their purchasing cost is very high. Additionally, ROVs' performance varies in the bad weather conditions such as clouds and winds.

In this way, visual methods with the use of advanced technology are highly regarded and safe as compared to other traditional methods for spillage detection. Additionally, the requirement of minimal supervision and durability to access inaccessible areas are the main reasons for their popularity. However, great effort has been making to the cost-effective and more sensible for underwater operations.

2.4 Performance Comparison of Leakage Detection Methods

As it has been earlier discussed three main methods external methods, interior methods, and visual methods for spillage detection on submarine pipelines as per literature cited and American petroleum Institute (API) performance required guidelines.

Table1: Performance Comparison of Pipeline leakage detection methods [20]

Particulars	**Exterior Method**	**Interior Method**	**Visual/ Biological Method**
Main Aspects	Leakage detection performed by sensing pipeline surrounding abnormalities	Leakage detected by monitoring inner flowing fluid properties such as mass, volume and pressure	Leakage detection performed by visual inspection, smelling odor, noise or vibration generation
Sensitivity to leakage	Depends on the sub method, (Medium-High)	Depends on the sub method, (Low-Medium)	Depends on the sub method, (Medium-High)
Detection Promptness	Low- Medium	Medium-High	High
Operating Cost	Medium- High	Medium-High	Very High
Limitations	Sensitive to random noise, false alarm	Leak size, performance affected by opening and closing valve, Computational Complexity	Performance affected by bad weather conditions

For evaluating the performance analysis of these methods various criteria have been considered such as leak localization, sensitivity, accuracy, purchasing cost and operational cost, false alarm rate, type of response. For ease of understanding, as shown in table 1 the essential criteria are discussed to compare the methods. Mainly principle of their operation, leakage sensitivity, detection promptness, operating cost, and limitations are featured in a way that they can be the main comparison can be understood. For example, detection promptness and operating cost can be evaluated at low-medium, medium-high, and high levels. All methods are not satisfying all aspects and they all have merits and limitations. However, these three methods have sub-methods that are not considered in this comparison.

2.5 Research Gap and Open Issues

According to the review of various pipeline spillage detection methods, the research gap and future work approaches are discussed in this section. The execution of the methods and sub-methods for pipeline leakage detection and localization varies depending upon their working principle, operating and purchasing cost, underwater environment conditions as discussed in detail before. However, American Petroleum Institute (API 1555) directives of sensitivity, accuracy, reliability, and adaptability are being followed by each facility in order to avoid major damages and causalities. Additionally, the oil and gas spillage rate of the pipeline is also a major concern of the pipeline company because it leads to maintenance as soon as possible to prevent the underwater environment. As a solution of this, more sensors can be deployed upstream and downstream along with the pipeline to monitor the spillage or oil contamination getting through it but costs very high at installation.

However, remote monitoring systems are beneficial as they provide information at a low cost and promptly through wireless communications technology. However, this kind of system is having design issues that require research attention including modality and coverage of sensing devices and spillage localization. Normally, sensors are deployed along with the pipeline to supervise the pipeline in steady-state conditions, and the changes in temperature, pressure, and vibration are counted as anomalous conditions of the pipeline. The accuracy performance of the sensors can be questionable if the leaks not within the coverage area of the monitoring system of the sensors. Wireless sensor networks (WSNs) have design issues that include fault- tolerance, optimal sensor node placement, sensor coverage, energy-saving routing, and energy harvesting. Additionally, there have been possibilities of sensor failure during their lifetime underwater where their lost function cannot be recovered. Eventually, this failure impacts the whole functionality of the network.

The sensor node placement influences the resource management and energy consumption of the Wireless Sensor Networks. The sensor coverage issue has been tried to resolve through the development of an analytical model and optimization approach in some studies, but still, research has been going to get a realistic model. Currently, the underground network has been expanding and the percentage of the communication network has been increased, it has become challenging to power for real-time sensing and data communication. The replacement of sensor node is also an expensive and infeasible task in the WSNs.

For continuous power requirements in the underwater weather, energy harvesters are introduced to acquire energy from the piezoelectric transducers through fluid flow, the

vibration of the pipeline surroundings, pressure of the water, etc., but the continuous and reliable energy source is still an open issue for the research work. Regarding leak localization, temperature variation in the pipeline surroundings affects the scalability and accuracy of the whole operation while the pipeline network is huge. Another important concern is that the leakage detection system gets the valid spillage and reduces the false alarm so the pipeline leakage detectors can attain the desired accuracy. Noise is a random phenomenon that affects spillage detection in a different way depending on the type of the system. This noise comes from system modeling, measurement system, data processing, and communications. However, noise can be reduced to a certain level by using signal filtering algorithms. The algorithms such as Savitzky-Golay, Ensemble, and Applet have been introduced to nullify the effect of signal distortion. Certain flow activities are good in decision-making activities, leak detection, pipeline maintenance, and leak localization and characterization. There are also data visualization tools.

In general, the main objective of the spillage detection system is to design a system with a real-time intelligent system for pipeline leakage and leak localization tasks. The underwater environmental factors and forces such as wave and current loading, depth and clarity level of the water, and changing environment require also research in so many areas.

2.6 Conclusion

In conclusion, the above presented a variety of researchers' work related to submarine pipeline leakage detection included their reviews of different methods of spillage detection, efficacy in underwater weather conditions, limitations, and efforts or thoughts to overcome

challenges. However, their work was lacking the consideration of all the available pipeline leakage detection technologies, the inclusion of advanced technologies, and their usage, approach towards AI and Machine Learning. Thus, the work presented in this thesis covers the gaps by presenting a SAUV approach for a submarine pipeline leakage detection system with the use of vision-based technology. The created model using this approach is a combination of the existing model and new emerging Computer Vision technology which fulfills most of the gaps in an affordable way. This is one of the most economical solutions for the offshore oil and pipeline industrial network.

CHAPTER 3

PROPOSED APPROACH: THEORETICAL BACKGROUND

3.1 Overview

Currently, new advanced technology is emerging in making the advancement of the Underwater Vehicle for various underwater applications in rescue, safety, oceanographic surveys, natural disaster warning system, and their research has been becoming a more interesting subject for scientists and entrepreneurs for decades. However, various methods are existing for spillage detection, vision-based methods especially underwater vehicles typically said "unmanned robots" are popular to fulfill the requirement and purpose of all underwater applications. Also, they overcome limitations of the interior and exterior methods through its advanced technological concept and use of machine learning algorithms.

Most subsea operations are conducted using a remotely controlled unmanned probe (ROV) operated by a human operator on a support vessel. Due to the complexity of the underwater environment, these tasks are often expensive, tedious, and require the continuous attention of a human operator to maneuver the robot in the presence of muddy seas and large fluid forces. Increasingly, over the years, there has been extensive research going on the development of autonomous underwater vehicles (AUVs). The main objective of the autonomous underwater vehicle is to perform each task automatically without human involvement/inspection in the underwater environment conditions. Over the past few years, optical and acoustic systems have been developed to cope with this objective through the

utilization of sensors, microcontrollers, and actuators. Currently, vision technology has been developing in the use of object detection and object recognition tasks through image processing. Visual-based systems are dependent on the noise of the underwater image acquisition process which is characterized by several mechanisms contributing to the degradation of the video signal. However, computer vision algorithms are developed to avoid background noise and other obstacles to maintain the smooth operation in a blurry and turbulent underwater environment.

In this chapter, the vision-based modeling approach with the utilization of SAUV has been introduced to perform spillage leakage detection for submarine pipelines. The operation of this model is representing the use of advanced computer vision algorithms for object detection and object recognition and remote underwater vehicle with a provision of working on auto/ manual mode. The objective of this approach to perform the spillage detection in prompt, accurate, sustainable, safe, and cost-effective for industrial use. Eventually, it is beneficial for the countries whose economy dependent on oil and gas industries. This model can work on both auto and manual, so this approach is called SAUV.

A SAUV is a self-propelled underwater vehicle that is called an unmanned underwater vehicle. It is an automatic or robot device that can be operated through a self-propelled system, controlled by the intelligent control system, and tilted in three dimensions. It falls under the category of mobile robots which involves actuators, sensors, microcontrollers to accomplish the desired task in safe and minimal human intervention. The utilization of these SAUVs has been increased in the recent years, as it is capable of pipeline tracking and ocean exploration. These SAUVs can function in a small, constrained, and hazardous area as they

are designed in a small and flexible way. For better performance of SAUV in energy consumption, dynamics, their bodies are designed to be streamlined.

The modeling approach has been introduced on based of computer vision-based system. In this system, the SAUV captures underwater images of spillage leakage detection and navigates itself along with the pipeline throughout the whole operation. The real-time images will be processed in order to main real-time control and operation. This chapter is organized in describing the specifications and features of the proposed SAUV. After that, we will move on to the design concept, block diagram, functionality of the SAUV. The presentation will include the description of all the material or parts being used and the software system controlling the whole operation.

3.2 Advanced Computer Vision-based Technology

In recent years, the interest of the scientific community in underwater computer vision has grown, taking advantage of the development of sensor technology or image processing algorithms. The main challenges of understanding underwater are due to the high cost of the devices, their complex configuration, and the signals and light propagation presented by the aquatic environment. In particular, the diffusion of light into the underwater environment suffers from phenomena such as absorption and scattering that strongly affect visual acuity. While underwater computer vision has been applied for observation, environmental monitoring, mapping, and terrain segmentation, the investigation of underwater objects has not been studied. In particular, accurate and robust object inspection and pose estimation are essential requirements for performing handling tasks. A robust detection method is

capable of correctly identifying different target objects under different experimental conditions. Once an image field corresponding to an object is found, its observation frame can be made into a single image stereo process. Currently, computer vision-based algorithms have been developed to perform many tasks in the area of science, mathematics, and engineering. The process of including acquire, process, analyze and understand images and videos through a vision sensor and camera is being done by the computer vision system. The system includes real-time image processing techniques through developed computer vision algorithms implementing in certain applications.

Computer vision is working on the theory of the extraction of information from images and videos. For this, the computer vision system takes the images and videos as input and extracts the useful information using decision-making algorithms. The image processing, pattern recognition, machine learning techniques are shared by both Artificial intelligence and computer vision system.

The tasks of computer vision system for object detection and classification includes as below:

(1) Object Recognition and classification

(2) Motion Detection and analysis

(3) Image and Scene Reconstruction

Image processing is mainly concerned with processing raw images by applying a sort of transformation by applying different types of filters. Generally, the objective of image processing is to improve the images taken by the camera or vision sensor and prepare them for certain tasks or application, while computer vision is used to describe and explain images.

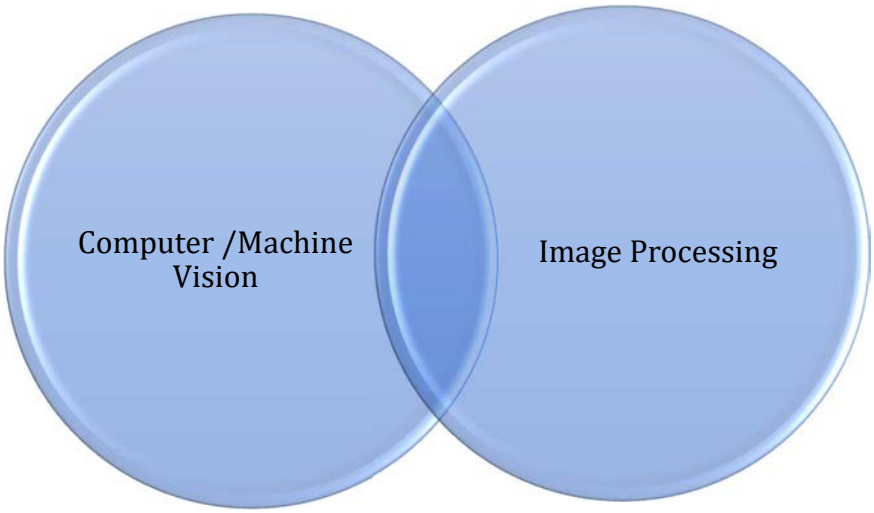

Fig. 6: Sharing concepts of Computer Vision System

For instance, noise reduction, threshold, and other components of image processing are applied to understand the image for a specific purpose or task.

Machine vision is the one scenario of the computer vision system which is being used in production and manufacturing lines. For example, in the chemical industry, it is being used to check the final product is whether clean and free of damage, sealed or not.

Computer vision is the one part of Artificial Intelligence that is used in subfields. The main objective of a Computer vision system is to replace the capacity of human vision. The computer Vision system can solve complex tasks intelligently through decision-making algorithms. For example, in Snapchat mobile application, the image or photo is visualized in desired copy through applying various filters. In all types and sizes of the companies, from the e-commerce industry to classic ones have been variously using a computer vision system. Currently, the exciting and challenging task of the computer vision system is object detection

in images and videos. Another task is image classification where images have been classified in the group where it belongs. The other objectives such as object identification, instance segmentation, object tracking also performed through a computer vision system.

3.2.1 Image Processing

As we discussed earlier, the extracted underwater images are processed further by developing different features such as intension, color, and segmentation in the image processing method. To achieve the goal, several steps shown below are considered to achieve the desired results. The procedure is as follows:

(1) Prepare color pictures of the input image.

(2) Adjusts the RGB image.

(3) Define the color of each pixel and define the color of the input image or background which is not related to the color of the object.

(4) Erase the unlinked area by replacing the color with all black.

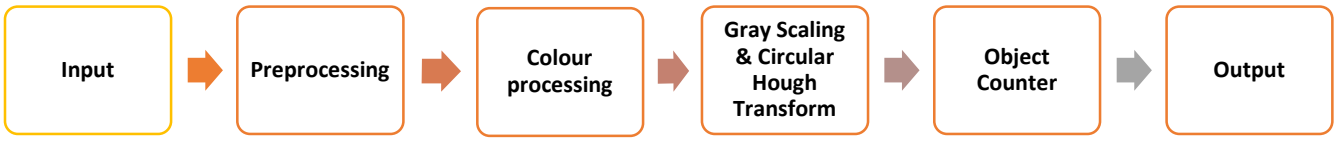

Fig. 7: Object detection block diagram

As shown in Fig. 7, the image is sent to the preprocessing block to set the image resizing to 320x240 pixels. Then, it follows straight to RGB compatibility and re-adjust the color and

background brightness and darkness of the object. Next, color processing is performed, irrelevant color removal is performed and mango color remains. The relevant pixels are removed by comparing the current pixel's RGB value with the mango's default RGB value. If the detected color is not present, change the current pixel's RGB value to 0 which is black. After color processing, the only matter left for this image is a transparent handle and blade that is colored like the handles. Here, the shape detection process is used to detect shapes rather than color detection. Before that, you need to behave in grayscale to remove the small pixel and perform a medium filter to smooth the image. In the middle filter, it will remove the small pixels and soften the images so that the edges of the objects are clean and neat. It will then switch to the binary icon and go through another object delete that removes binary objects that are less than 200 pixels in the group of objects.

3.2.2 Image Preprocessing for underwater object detection

Image preprocessing is a process that includes several components such as image filtering, image fields, shape processing, and edge detection. The method chosen is more focused on practical use, as it is primarily intended to capture the points of the underwater pipeline in the picture. A median filter (7X7) is selected to smooth the image. The method based on the iterative optimal threshold is chosen to segment images. Two morphological operations (opening and closing) are selected to eliminate the protrusions and fill the holes. A Sobel operator is used to extract the contours of the pipeline. Utilizing the above methods, the results are shown in Fig. 8.

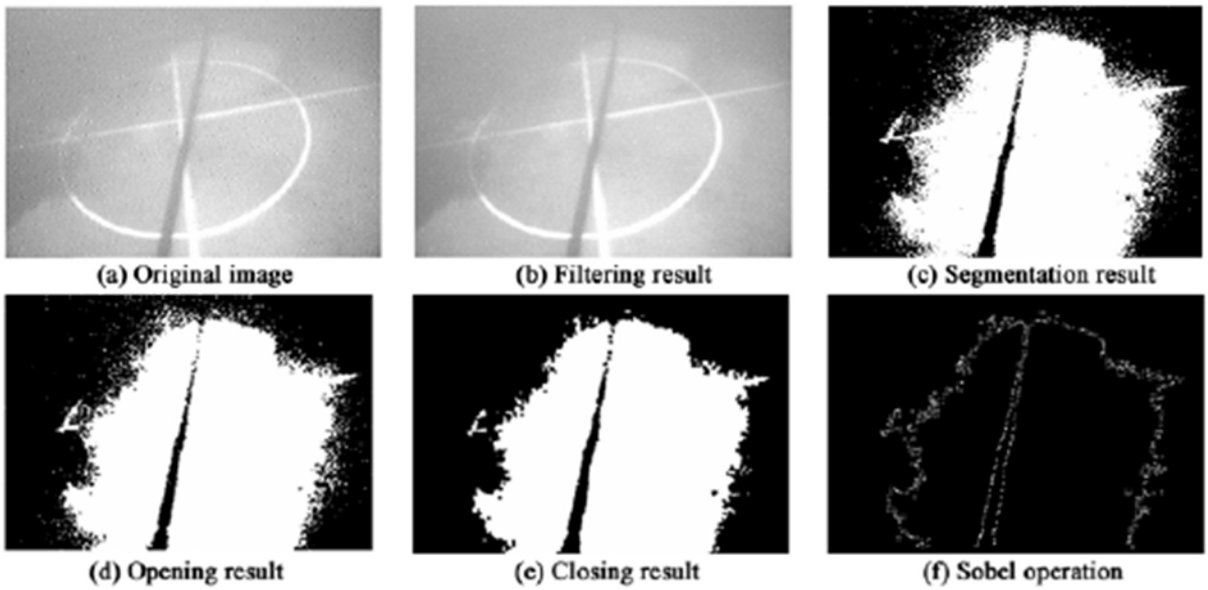

Fig. 8: Image processing of pipeline edge detection [40]

In this way, image preprocessing is mainly working on the input image or original image and apply different kinds of filter, add and remove noise and finally segment the image for the desired object.

3.2.3 Canny Edge Detection

Canny Edge Detector is the most popular method as it is the most optimal in finding edges with good detection and good localization. It uses a multi-stage algorithm to detect wide edges in the images. This technique which was developed by John F. Canny can be explained by following the below steps:

A. Noise reduction

B. Gradient Calculation

C. Non-Maximum Suppression

D. Double threshold

E. Edge tracking by Hysteresis

The above all steps are discussed below in the detail to get overall idea of the edge detection of the original image.

A. Noise Reduction:

In the first step for edge detection, the noise of the image is filtered out. The input image is converted into grayscale with adjustment of contrast and brightness therefore image becomes blurry to remove the noise. Generally, a Gaussian filter is used to remove the noise from the image. The method of convolution of images with a Gaussian kernel (3x3, 5x5, 7x7, etc.) is used for this. The kernel size depends on the expected blurring effect. In principle, the smaller the core size, the less noticeable the blurring. In our example, we will use a 5 x 5 Gaussian kernel.

B. Gradient Calculation:

The gradient calculation step finds the edge intensity and direction of the image by calculating the edge of the image using the edge search operators. The edges correspond to a change in the intensity of the pixels. To find it, the simplest way is to apply filters that illuminate this intensity change in both directions: horizontal (x) and vertical (y). When the

image is smoothed, the derivatives Ix and Iy with respect to x and y are computed. It can be expressed by involving with Sobel's kernels Kx and Ky respectively:

$$K_x = \begin{pmatrix} -1 & 0 & 1 \\ -2 & 0 & 2 \\ -1 & 0 & 1 \end{pmatrix}, K_y = \begin{pmatrix} 1 & 2 & 1 \\ 0 & 0 & 0 \\ -1 & -2 & -1 \end{pmatrix} \quad \text{.....(2)}$$

The magnitude G and $\boldsymbol{\theta}$ calculation is as below:

$$|G| = \sqrt{{I_x}^2 + {I_y}^2} \quad \text{.....(3)}$$

$$\theta(x, y) = arctan\left(\frac{I_x}{I_y}\right) \quad \text{.....(4)}$$

Gradient intensity levels are between 0 and 255 and are not uniform. The final edge must have the same intensity (that is, white pixels = 255).

C. Non - Maximum suppression:

To get the final image in a thin image, in this step the Non- maximum suppression is applied to thin the images. In this technique, the algorithm moves through all points of the gradient intensity matrix and finds pixels with the maximum value in the edge directions.

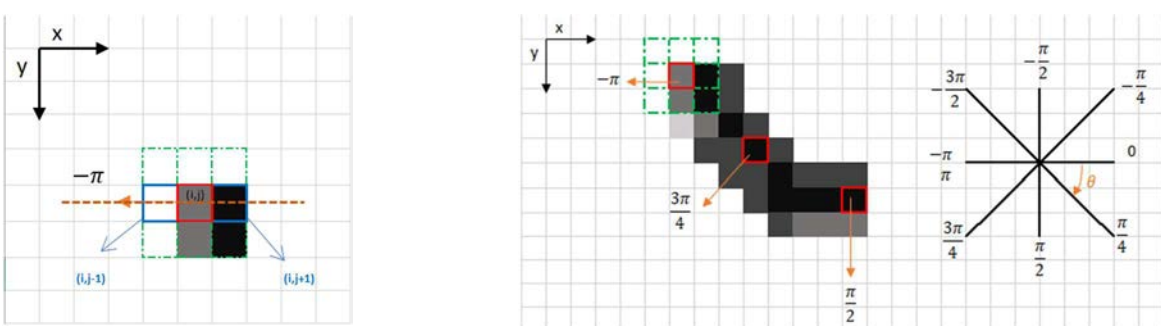

Fig. 9 & Fig. 10: Non – Maximum Suppression Example [1]

For instance, as shown in the left side Fig. 9, the red box in the upper left corner of the image above represents the intensity pixels of the gradient intensity matrix being processed. The corresponding edge direction is indicated by an orange arrow with an angle of -pi radians (+/- 180 °). The direction of the border is the orange dotted line (left to right horizontal). In the example above, pixels (i, j) are being processed and pixels in the same direction are highlighted in blue (i, j-1) and (i, j + 1). If one of these two pixels is much more intense than the process, only the extreme remains. The pixel (i, j-1) looks more intense because it is white (value 255). Therefore, the intensity value of the current pixel (i, j) is set to 0. If there are no pixels in the direction of the edge that have strong values, the value of the current pixel will be retained.

Each pixel has 2 main criteria (edge direction in radians, and pixel intensity between ((0-255)). There are maximum pressure measures based on these outputs: 1. Create an initial matrix from 0 to the same size with a real gradient intensity matrix. 2. Identify the direction of the edge based on the angle value from the angle matrix. 3. Check that the pixel in the same direction is currently higher than the processed pixel. 4. Return the executed image with the maximum suppression algorithm.

D. Double Threshold:

The purpose of the double square phase is to identify 3 types of pixels: strong, weak, and non-existent: strong pixels are hard pixels and we believe that they contribute to the final edge. Weak pixels are pixels that have a value of intensity that is not strong enough to be considered, but not small enough to be considered irrelevant to detect the edge. Other pixels

are considered infinite. Now you can see what double thresholds are: High threshold is used to indicate strong threshold (high threshold intensity) while Low threshold is used to identify unrelated pixels (low threshold intensity).

E. Edge Tracking by hysteresis:

Based on the threshold results, hysteresis consists of converting weak pixels into strong pixels, if and only if at least one of the executed pixels is strong.

3.2.4 Hough Transform

After edge detection, Hough Transform is performed to detect desired shape or region of interest (ROI). Usually, regions of interest may have different sizes and shapes, so an algorithm that can find these shapes within the image and recognizes the objects as per predefined parameters is needed. Hough transform, which fulfills this purpose is mostly used for object recognition. This method performs detection of irregular instances of objects in a pre-defined set of shapes through a voting procedure on the binary images converted from gray-scale images.

Hough Transform (HT), named after Paul Hough, who patented the method in 1962, is a powerful global method that performs the conversion between Cartesian space and a parameter space in which a straight line (or some other boundary formulation) can be defined. Let us consider the case where an image consists of straight lines. We first find that

for each point (xi, yi) in this diagram, all straight lines passing through this point satisfy equation 5 for different values of line slope and intersection point (m, c), shown in Fig. 11.

$$\boldsymbol{y_i = mx_i + c} \quad \text{.....(5)}$$

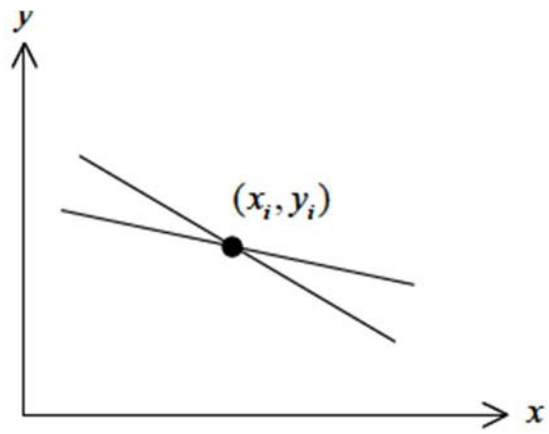

Fig. 11: Line Representation in X-Y plane

Now if we invert our variables and instead treat the value (m, c) as a function of the coordinates of the image point (xi, yi) then equation 5 becomes:

$$\boldsymbol{c = y_i - mx_i} \quad \text{.....(6)}$$

Equation 6 describes a straight line on the plot of c vs. Shown in Fig. 12

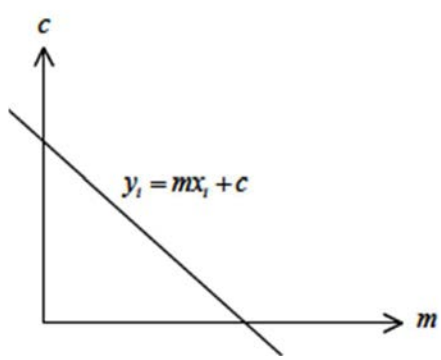

Fig. 12: The domain (m, c)

At this point, it is easy to see that each different line through the point (xi, yi) corresponds to one of the points on the line in the (m, c) space. Now, consider two pixels P1 and P2, which lie on the same line in the (x, y) space. For each pixel, we can represent all the possible lines through it by a single line in the (m, c) space. Thus, a line in the (x, y) space that passes through both pixels must lie on the intersection of the two lines in the (m, c) space, which represents the two pixels. This means that all pixels which lie on the same line in the (x, y) space are represented by lines that all pass through a single point in the (m, c) space, see Fig. 13 and Fig. 14.

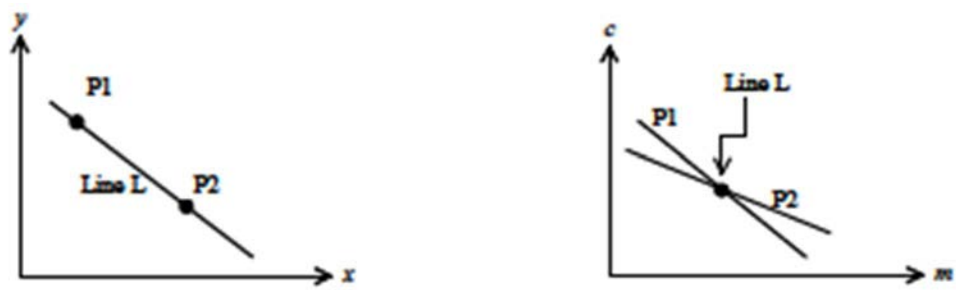

Fig. 13 and 14: The plotting of points P1, P2 on the (m, c) plane

After the discussion above, we can now describe the algorithm for finding the lines in the images. The steps are:

(1) Find all the edge points in the image using any suitable edge detection technique.

(2) Quantify the space (m, c) as a two-dimensional matrix H with corresponding quantification levels.

(3) Start the matrix H to zero.

(4) Each element of the matrix H, (mi, ci) corresponding to the edge point increases by 1. The result is a histogram or matrix of votes showing the frequency of edge points corresponding to a few (m, c) values (i.e., lying on a common line).

(5) The threshold is determined by the histogram H when only the elements with the largest values are taken. These elements correspond to the lines in the original image.

The advantage of Hough transformation is that the pixels in a line cannot match everyone. This can be very useful when trying to find short-pause lines due to noise or when things are partially covered.

For Circular Hough Transform, a following procedure is followed:

The equation of the circle is:

$$r^2 = (x-a)^2 + (y-b)^2 \quad \text{.....(7)}$$

Where a and b are the coordinates of the center, and r = radius of the circle. The circle can be represented in a parametric:

$$x = a + r\cos\theta \quad \text{.....(8)}$$

$$y = b + r\sin\theta \quad \text{.....(9)}$$

Unlike linear HT, CHT3 relies on parameters that require more computation time and more memory, which increases the complexity of extracting information from our image. For simplicity, most CHT programs set the radius to a fixed value (hard-coded) or give users the option to set the range (maximum and minimum) before running the application. For each edge point, a circle with that point is drawn as the origin and radius r. The CHT uses an array

(3D) with the first two dimensions Fig. 15 representing the coordinates of the circle and the radius of the last third. The accumulator values increase each time a circle is drawn with the desired radius at each edge point. The accumulator counts the number of circles that pass through the coordinates of each edge point and votes to find the highest number. The middle coordinates of the circles in the images are a large number of coordinates shown in Fig. 16.

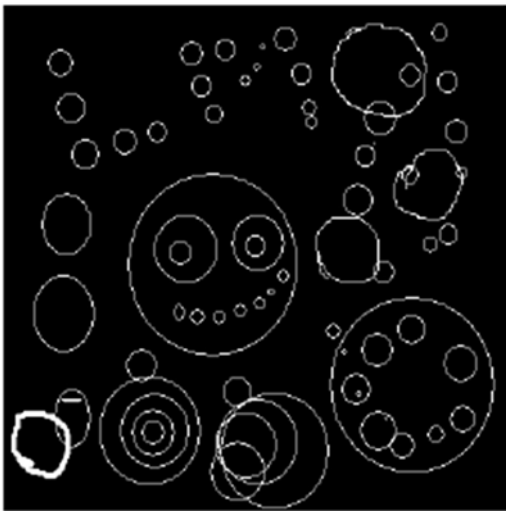

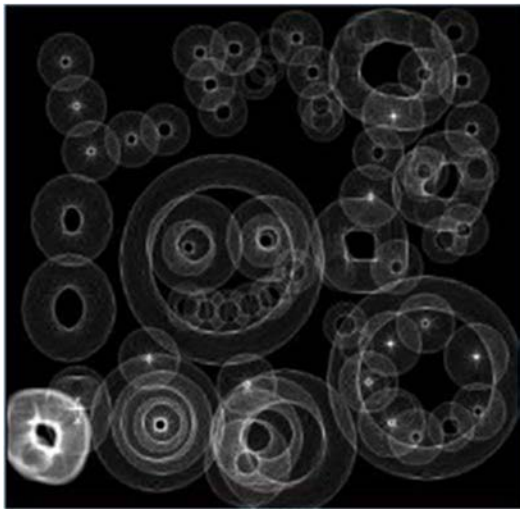

Fig. 15: Input Image – After edge detection and Fig. 16 Image after Voting [13]

The advantage of Hough transformation is that the pixels in a line cannot match everyone. This can be very useful when trying to find short-pause lines due to noise or when things are partially covered.

3.3 Conclusion

As we discussed above, image processing, computer vision, Canny edge detection, and Hough Transform are the key concepts to make the proposed model for submarine pipeline leakage detection. We will see their implementation in the next chapter in the modeling approach.

CHAPTER 4

PROPOSED APPROACH: SAUV VISION-BASED SYSTEM

4.1 SAUV Concept

The main concept of the SAUV is vision-based tracking and taking images of the blob which is created in the underwater environment. The SAUV is also capable of the switch itself in the manual and auto mode. It can dive into the programmable depth of the water and follow the pathways to conduct the survey. The survey of the SAUV will capture the blob images using one camera. When it captures blob images, SAUV stops tracking for a while and continues to follow the path by vision tracking. During the entire mission, it captures images and stores those images in the memory.

At starting position, the SAUV will be operated by a joystick through an umbilical cable in the underwater environment, and after balancing it will be switched to auto mode. Balancing SAUV is the most important task while tracking. During the whole operation, line tracking along with the pipeline, balancing in an underwater environment, and blob detection during tracking are the main three objectives.

4.1.1 Architecture

The main aspects of the SAUV are microcontroller assembly and SAUV vehicle in this proposed model as shown in Fig. 17. The Raspberry Pi is a microcontroller that controls the entire mission as well as processes the computer vision algorithms to enable the vision-based system. The entire control system controls the 6 thrusters based on the waypoints of

the mission plan and as well as feedback from the computer vision algorithm. The electric speed controller (ESC) works as an interface that takes the control signal from the microcontroller and delivers the proportional high-power current from the battery to the thruster motors. The gyroscope and leak detector are the inputs to the microcontroller. The Pi camera is also acting as an input to the microcontroller. The LED lights are utilized for lighting the camera scene while natural light is not sufficient for the operation. The images captured by the Pi camera are stored in SD card memory by the CPU. A 12-volt Lithium battery packs to power the entire system.

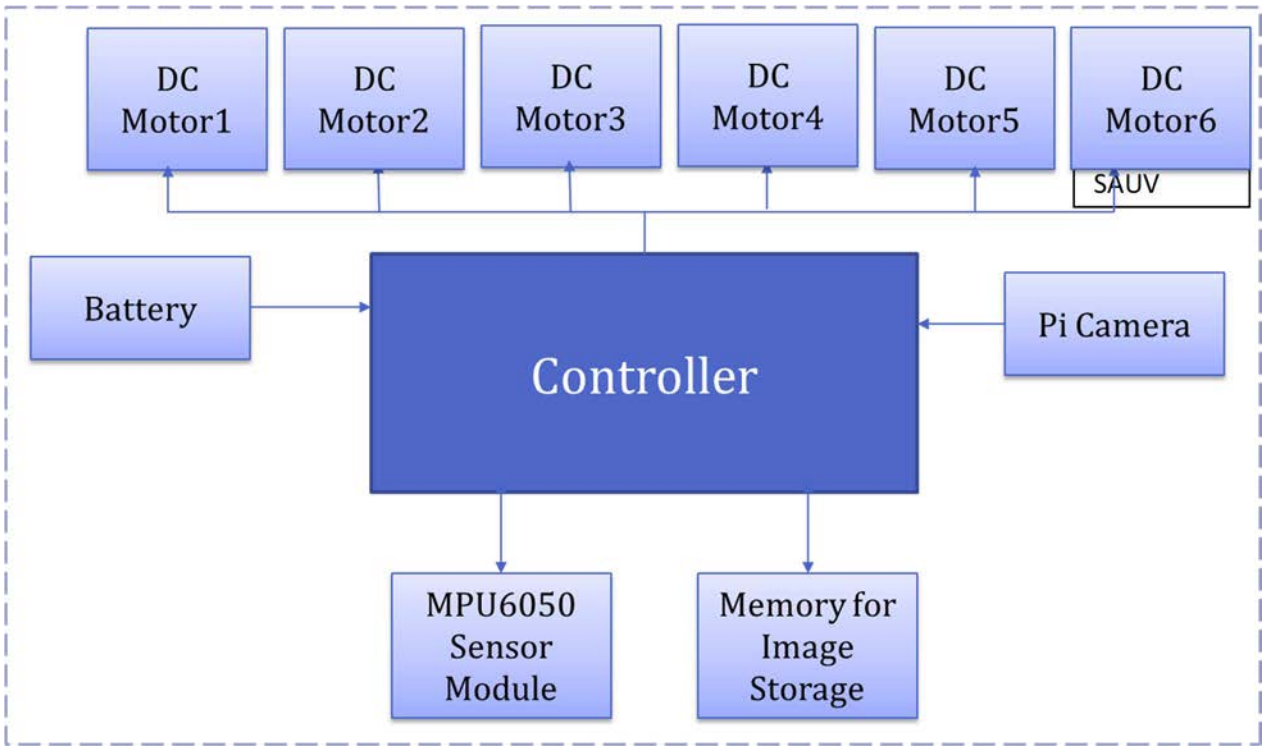

Fig. 17 Block diagram of proposed SAUV approach

The Remote Operated Vehicle (ROV) has a waterproof central main cylinder with a transparent dome at the front. The dome on the front will be made of acrylic material to bring transparency to the front view of the vehicle for the front camera. There will be two small auxiliary cylinders on each side that can be used to carry additional batteries to extend the

vehicle's endurance on a single dive mission. There will be 6 thrusters to provide 4 degrees of freedom, namely Surge, Sway, Heave, and Yaw for heading change. The center cylinder contains all electronic systems and the main battery required for the operation of the vehicle. There is a skid underneath the vehicle to properly position and transport the vehicle on the ground and avoid hitting or damaging the camera below as it approaches the seabed.

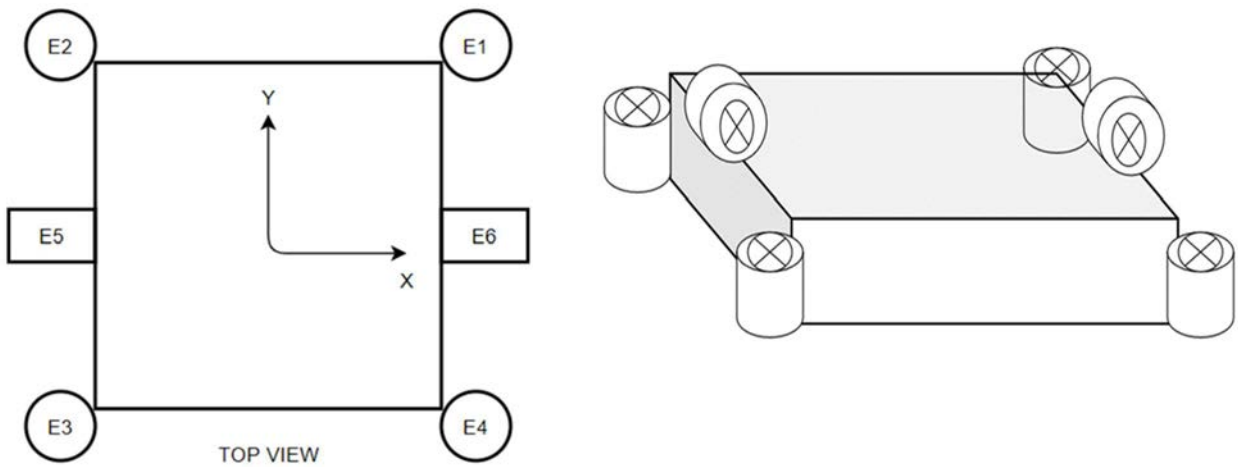

Fig. 18 Arrangement of DC Motors

Fig. 18 shows the arrangement of ESC motors. There are 6 motors M1, M2, M3, M4, E5, and E6 are arranged in that manner so the unbalancing possibilities of SAUV in 4 ways can be eliminated. E5 and E6 are mainly functioning to drive the SAUV in left and right-side control. In the whole arrangement, the X and Y axis are considered for balancing the purpose of SAUV in both directions.

The purpose of this design is to perform the three main tasks:

(1) SAUV balancing during the whole operation

(2) SAUV line tracking

(3) The spillage detection during tracking.

The shape and design features of the c are being done in such a way that they can support the objective of the whole operation. The underwater environment is blurry and there is an influence of ocean currents, and turbulence of the water affect the functionality of the operation. To minimizing these barriers in the functioning of SAUV the features are designed.

4.1.2 System Components

The front SAUV dome is made of acrylic material to provide transparency for the front camera to view the front of the vehicle. The rest of the cylinder is made of aluminum material. The bottom cover of the camera is made of acrylic material. The materials used in the whole operation are described as follow:

A. Brushless DC Motors

Fig. 19 Brushless DC Motors

In this operation, we are using 1000 KV and 12 V brushless DC motor (Fig.19) The brushless DC motors are utilized in immerse facilities such as automobile, automation, consumer electronics, medical and industrial applications. Brushless DC motors (BLDCs) are also known as electronic rectifying motors. The rotor does not have a brush and is electronically commutated at a specific rotor position. BLDC motors are permanent magnet synchronous motors with a unique counter electromotive force waveform that can behave like brushed DC motors. BLDC motors do not operate directly from DC voltage sources. However, the basic operating principle is the same as for DC motors. A brushless DC motor has a permanent magnet rotor and winding stator, while the BLDC motor essentially rotates the DC motor. The brushes and commutator are removed and the windings are connected to the control electronics. Control electronics alter the actuator of the commutator and promote proper winding, the winding is excited in the rotating pattern of the stator, the radiation stator winding causes the rotor magnet to change, and the alignment of the rotor-stator. The brushless DC motor is an ideal choice for applications that require high reliability, high efficiency, and a high power-to-volume ratio. Generally speaking, the BLDC motor is considered a high-performance motor, capable of delivering great torque over a wide range of speeds. Because of all these advantages, brushless DC motors are widely used in modern devices that require low noise and heat, especially in devices that operate continuously. This can include washing machines, air conditioners, and other consumer electronics. They can even be the main source of power for service robots, which require very careful force control for safety reasons.

B. Electronic Speed Controllers

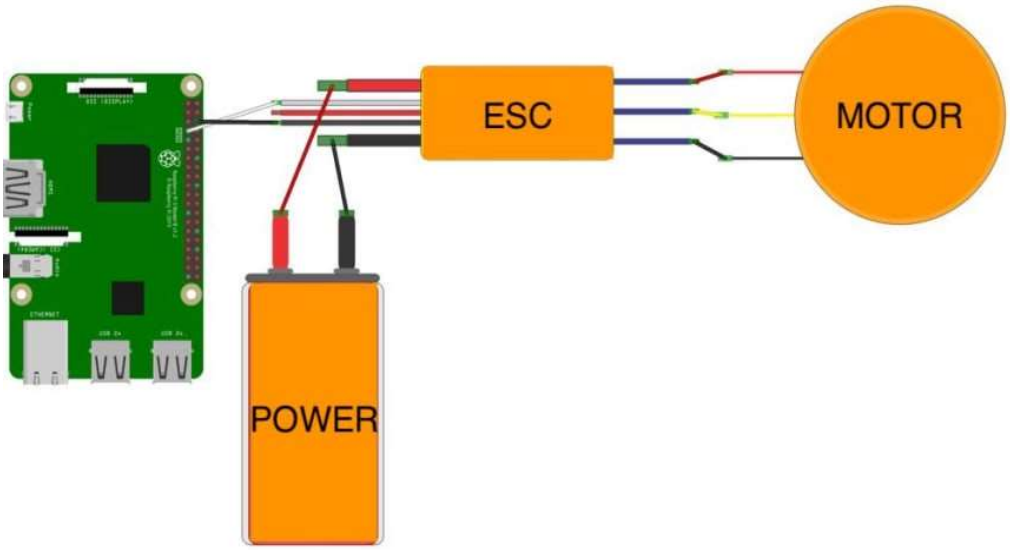

Fig. 20 Bi-directional Control through ESC and controller

Motors can be rotated in either direction, i.e., clockwise and clockwise, using bi-directional controllers connected to the Raspberry Pi board. The electronic Speed Controller (ESC) shown in Fig. 20 is an electronic circuit that is used to change the speed of an electric motor and its path, and also to act as a dynamic brake. It is often used on radio-controlled models. There are those that run electrically, with this modification commonly used for brushless motors that provide an electrically designed 3 phase low voltage power source for the motor. A regulator can be a separate unit that the gas sinks into the receiver's control channel or connects to the receiver itself, as are most toy-quality R / C vehicles, some R / C manufacturers that own entry-level vehicles, containers, or aircraft. They use electronics that connect the two in the same circuit board. The electronic speed control follows the speed reference (derived from the throttle lever, joystick, or other manual input) and changes the switching speed of the field-effect transistor (FET) network. By adjusting the duty cycle or

switching frequency of the transistor, the motor speed changes. Rapid switching of transistors is what causes the motor to emit its characteristic high pitch whine, particularly noticeable at low revs. Brushed DC motors and brushless DC motors require different types of speed control. You can control the speed of the brush motor armature by changing the voltage. (Indirectly, motors with electromagnet field windings instead of permanent magnets can also control speed by adjusting the current strength of the motor field.) Brushless motors require different operating principles.

The speed of the motor changes by adjusting the time of the current pulses delivered to multiple turns of the motor. Brushless ESC systems generate a three-phase AC power source, such as a VFD variable frequency drive, to drive a brushless motor. Brushless motors are popular with wirelessly controlled airplane enthusiasts because of their efficiency, power, longevity, and lightweight compared to traditional brush motors. Brushless DC motor controllers are much more complex than brush motor controllers. The correct phase depends on the motor winding which needs to be considered in the ESC. Normally, the EMF returned from the motor winding is used to detect this winding, but there are variations in magnetism (Hall effect) using sensors or photodetectors. Computer-programmable speed controls typically have user-specified options that allow you to set low-voltage cutoff limits, timing, acceleration, braking, and direction of rotation. Reversing the direction of the motor can also be achieved by switching any two of the three leads from the ESC to the motor. Electric speed controllers can be a stand-alone unit that plugs into the receiver's throttle control channel or connects to the receiver itself, as is the case with most toy quality R / C vehicles. Some R / C manufacturers that install proprietary hobby electronics in their

interior vehicles, aircraft, or airplanes use aircraft electronics that combine the two into a circuit board.

C. Battery (LiPO)

Fig. 21 LiPo Battery for used in SAUV

The SAUV uses electrical power from an onboard battery to power its various components. The power source we used was a 12V DC lithium polymer battery shown in Fig. 21. The actual voltage produced by a fully charged LiPo battery is approximately 13 VDC, which feeds directly into the thruster motors via ESC. The low voltage supply required for the controller board is obtained using a step-down DC-DC converter. The vehicle is designed to operate autonomously in untethered condition for 2 hours.

D. Pi Camera

A Pi camera is used for image capture as well as image tracking and processing. The entire pan/tilt mechanism and camera are housed in the hemispherical acrylic dome of the vehicle's main cylinder. This fully enclosed design offers a 180-degree view of the camera

and is still waterproof. The pan and tilt function gives the camera a wider field of view. Light-emitting diodes (LEDs) on the circuit board are used to illuminate the underwater environment. The end cap has two O-ring grooves to keep the case watertight.

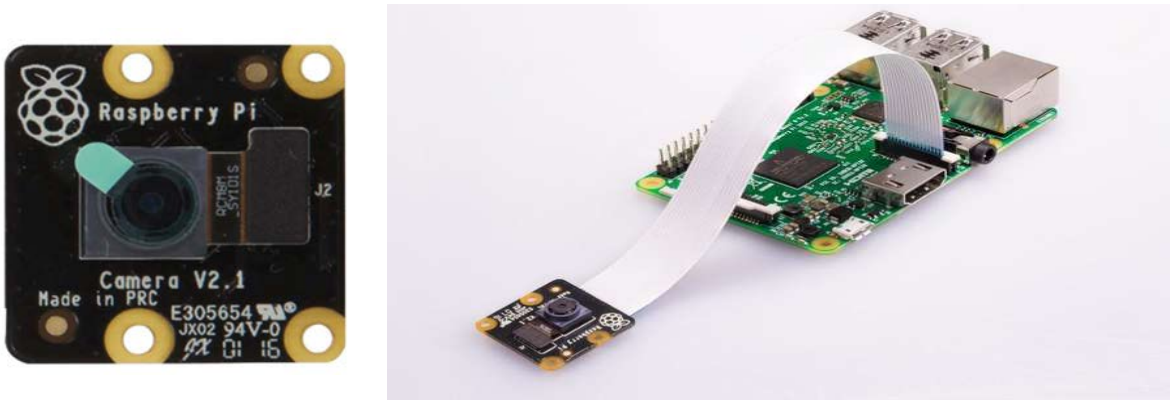

Fig. 22 Pi Camera (NoIR V2)

As shown in Fig. 22, the NoIR Pi Camera is used here for capturing the high-resolution image in nighttime or dark underwater environment. Usually, cameras are working in the daytime and a clear environment provides better results as compared to dark and nighttime. Here, considering the underwater environment situations and eliminate the barriers, a NoIR camera is used. It is a “Non-infrared” camera which provides the same result as daytime in dark and night time. This 8MP IR (Infrared) camera module can record 1080p videos and still images and connect directly to your Raspberry Pi. Just like the Raspberry Pi camera without the IR version, connect the ribbon cable provided with your Raspberry Pi's CSI connection (camera serial interface), start the latest version of Raspberry and you go. Weighing 25mm x 20mm x 9mm and over 3 grams, this board is very small, making it perfect for mobile or other small apps where you need to look in the dark. The sensor has a base resolution of 5 megapixels, with a fixed focus lens onboard. The Marrow supports static

images with 3280 x 2464 pixels and also supports videos with 1080p30, 0, 720p60 and 640x480p90.

E. Control Board (Raspberry Pi)

Raspberry Pi is the controller of the SAUV which controls all inputs and outputs during the whole operation. The main features of the Raspberry Pi are as below:

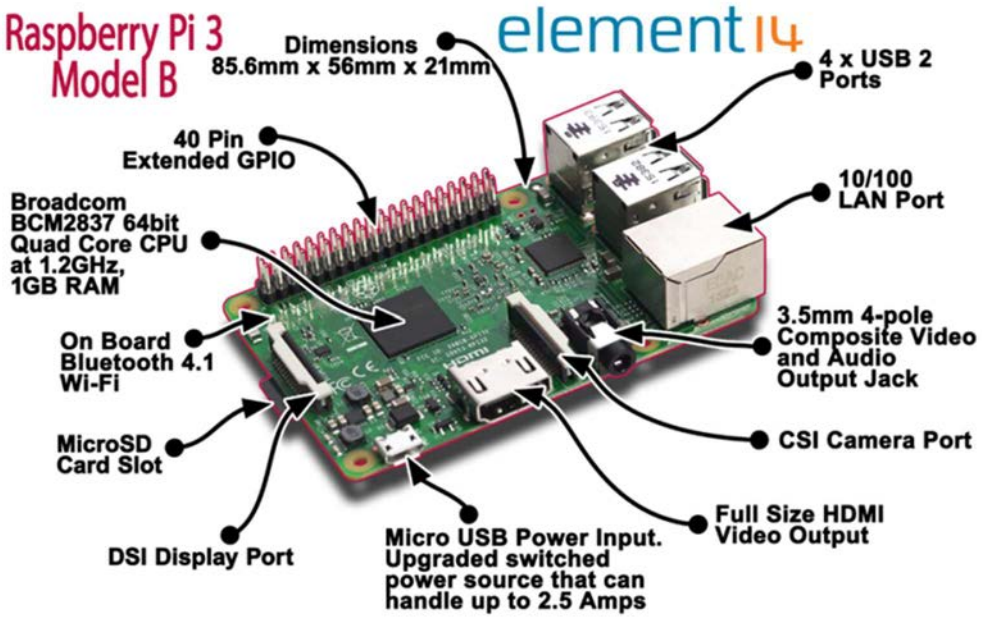

Fig. 23a Raspberry Pi 3 – Model B

As shown in Fig. 23a a Raspberry Pi controller has been selected for use due to its more complex design for the full processor and the software drivers and libraries installed on it. The Ethernet port on the R-Pi board allows remote communication with semi-automatic underwater over an Ethernet cable during the debugging process. In addition to this, the R-Pi board has four USB ports that allow you to connect a standard low-cost USB camera to the board for vision-based tracking. In addition, USB cameras are cheaper and smaller than Ethernet-based cameras. The Raspberry Pi software is easy to manage and easy to keep up

to date. The board can run a standard Linux OS on the board, so some additional features and standard programming libraries are available. The board is programmed in Python, which speeds up unit testing and makes it easy to manage large codebases, rather than C programs. The Ethernet port on the Raspberry Pi board allows the AUV to update the code underwater using the remote login feature. This allows for quick corrections and repetitive improvements when testing SAUV underwater.

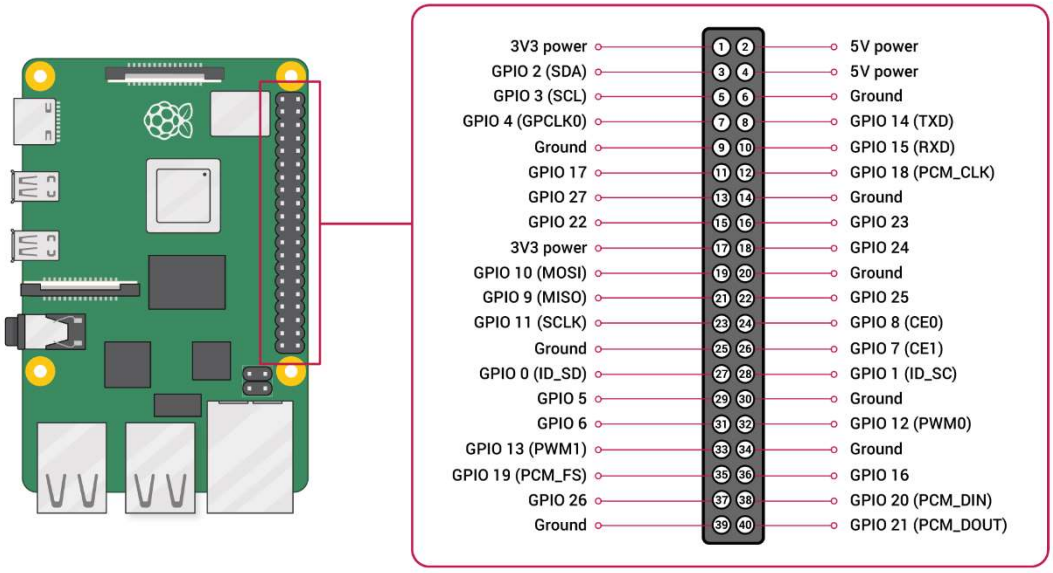

Fig. 23b Raspberry Pi-GPIO

This block diagram describes models B and B +. Models A, A +, and P Zero are similar but lack Ethernet and USB hub components. The Ethernet adapter is internally connected to an additional USB port. For models A, A +, and P Zero, the USB port is directly connected to the system (SOC) on the chip. The USB / Ethernet chips of P1 model B + and later models include a 5-port USB hub, four of which are available, but P1 model B offers only two. On Pi Zero, the USB port is also directly connected to the SOC but uses a micro-USB (OTG) port. Unlike all

other Pi models, the 40-pin GPIO connector is omitted with pin 0, and the through-holes available for sale are only in pin positions.

This is the P Zero WH remedy. Processor speeds range from 700 MHz to 1.5 GHz for the PI3 Model B + or P4 to 1.4 GHz. 6 Non-board memory ranges from 256 MB to 1 GiB in random access memory (RAM), of which 8 GB is available on the Pi 4 operating system and program memory. The board has one to five USB ports. For video output, HDMI and composite video are supported, with a standard 3.5mm tip-color-sleeve jack for HD video output.

A powerful feature as shown in Fig. 23b of the Raspberry Pi is the row of GPIO (General Purpose In / Out) pins along the top edge of the board. The 40-pin GPIO header is found on all current Raspberry Pi boards (not implemented on Pi Zero and Pi Zero W). Before the Pi1 Model B + (2014), the board consisted of a short 26-pin header.

F. MPU6050 Module

In this method, the MPU6050 module has been used for SAUV balancing task. The introduction, functionality, and interface has been discussed here.

The MPU6050 sensor module shown in Fig. 24 is an integrated 6-axis motion tracking device. A 3-axis gyroscope, 3-axis accelerometer, digital motion processor, and temperature sensor are mounted on one IC. Inputs from other sensors such as 3-axis magnetometers and pressure sensors can be accepted via an additional I2C bus. An external 3-axis magnetometer can be connected to provide a complete 9-axis motion fusion output. Microcontrollers can communicate with this module using the I2C communication protocol. Various parameters

can be found by reading the value from the address of a particular register using I2C communication. Gyroscope and accelerometer readings along the X, Y, and Z-axis are available in two's complement format. Gyroscope readings are expressed in degrees per second (d/s).

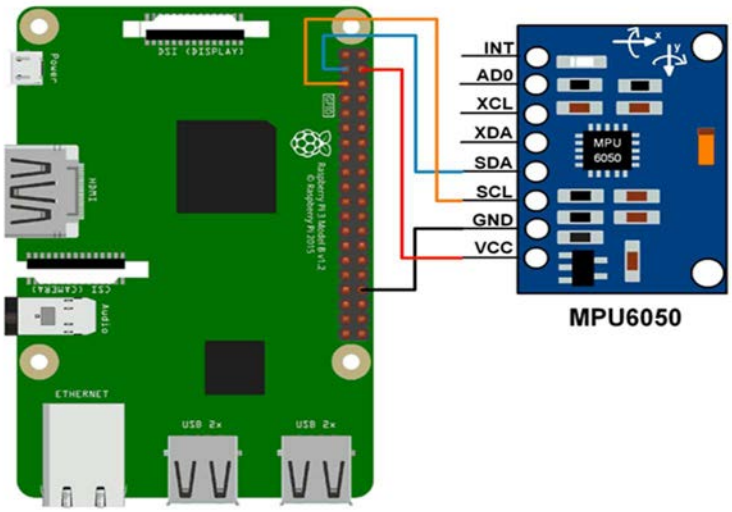

Fig. 24 MPU 6050 with controller

Accelerometer readings are shown in grams. The MPU6050 includes a 3-axis gyroscope with Micro Electro Mechanical System (MEMS) technology. It is used to determine the rotation speed along the X, Y, Z axes as shown in Fig. 25.

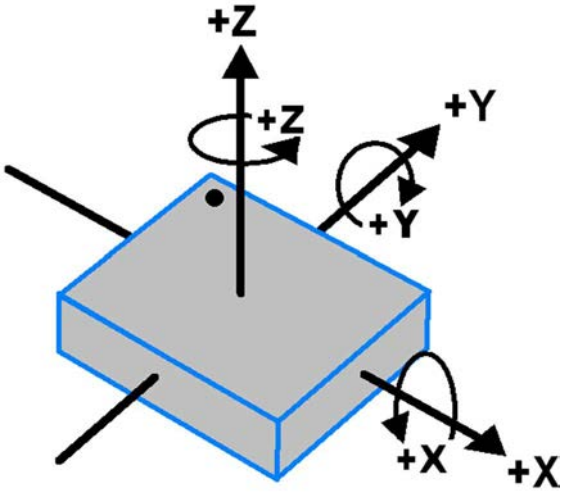

Fig. 25 MPU – 6050 Orientation and Polarity Rotation

When the gyro rotates around one of the detected axis, the Coriolis effect causes vibrations that are detected by the MPU6050's MEM. The resulting signal is amplified, demodulated, and filtered to produce a voltage proportional to the angular velocity. This voltage is digitized using a 16-bit ADC and samples each axis. The total output range is +/- 250, + / -500, + / -1000, + / -2000. It measures the angular velocity along each axis in degrees per second.

The MPU6050 includes a 3-axis accelerometer with microelectromechanical technology (MEM). It is used to detect the angle of inclination or inclination along the X, Y, and Z axes as shown in Fig. 26.

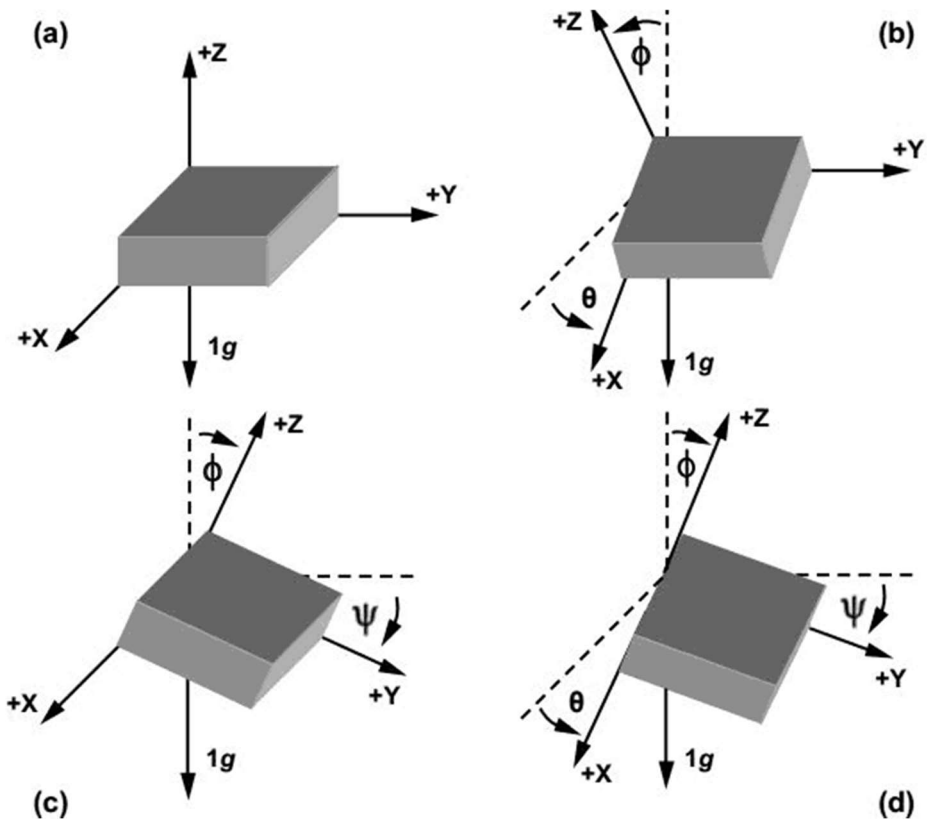

Fig. 26 Accelerometer motion in 3 - Axis

Acceleration along the axis is applied on a large scale. This displacement of the dynamic plate (mass) balances the discriminating signal, resulting in the sensor being recovered. The output dimension is proportional to Excel. A 16-bit ADC is used to achieve digitized output. The full-scale acceleration range is +/- 2g, +/- 4g, +/- 8g, +/- 16g. It is measured in units G (force of gravity). When the instrument is placed on a flat surface, it will measure 0g on the X and Y axis and + 1g on the Z-axis.

Accelerometer values in g (g force)

Acceleration along the X axis = (Accelerometer X axis raw data/16384) g.

Acceleration along the Y axis = (Accelerometer Y axis raw data/16384) g.

Acceleration along the Z axis = (Accelerometer Z axis raw data/16384) g.

Gyroscope values in °/s (degree per second)

Angular velocity along the X axis = (Gyroscope X axis raw data/131) °/s.

Angular velocity along the Y axis = (Gyroscope Y axis raw data/131) °/s.

Angular velocity along the Z axis = (Gyroscope Z axis raw data/131) °/s.

4.1.3 Vision-based Tracking

Vision-based tracking is an operation to keep the tracking of SAUV along with the pipeline while spillage detection. The detailed procedure is as follows:

The tracking of the SAUV along with the pipeline is proposed in Fig. 27 uses the image processing and feature extraction techniques on the images taking by the Pi camera while

diving underwater. There is a white line drawn underneath the pipeline, so the SAUV will keep following it and track itself along with the pipeline.

The real-time images of the white line will be taken by the SAUV during its movement in the water. The instantaneous images will be scanned for matching features by the feature matching computer vision algorithm. The feature is compared to the database pre-indexed with the line features. Until a match is found each acquired image is scanned for matching features. Once a line is found as permission plan input, then the line is tracked by the SAUV standard vision tracked algorithm and the vehicle thrusters are also controlled to follow the line and keep the camera close to the line as much as possible. Once tracking is lost i.e., the line is not visible in the camera image then feature matching again starts and continues.

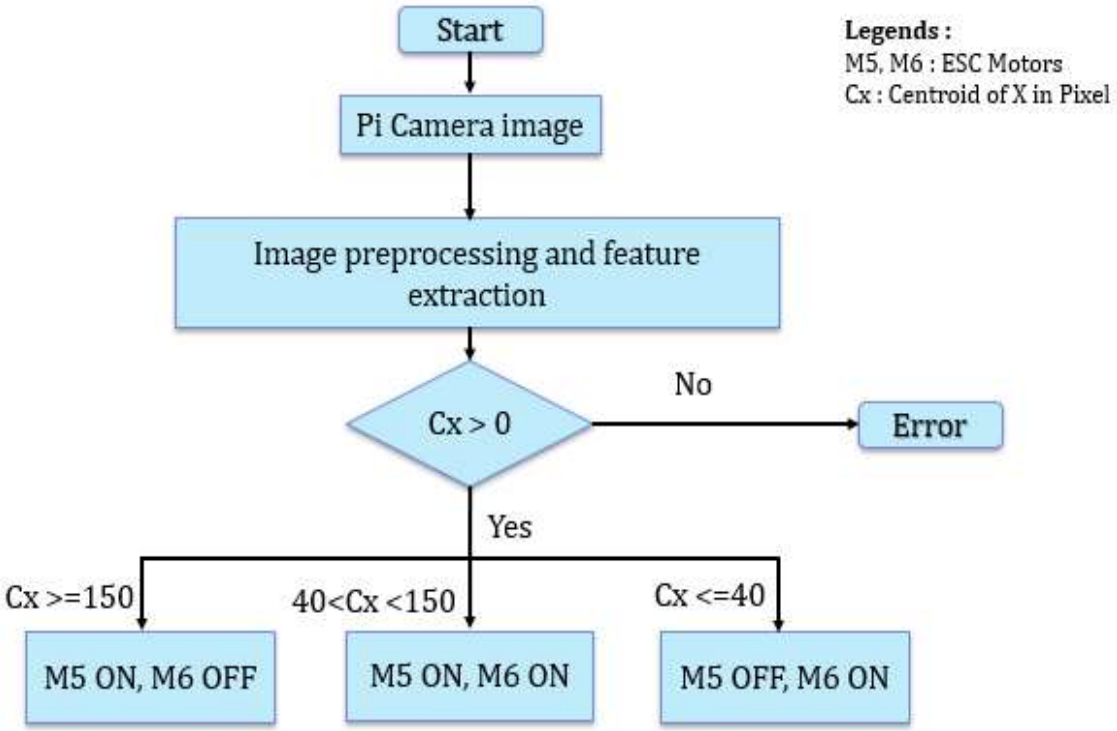

Fig. 27 Vision- based tracking

To find out the Cx (Fig. 28) which is the centroid of the large contour area, the image frame which has the largest contour area is divided in the center into two parts to find out the centroid of the large contour area.

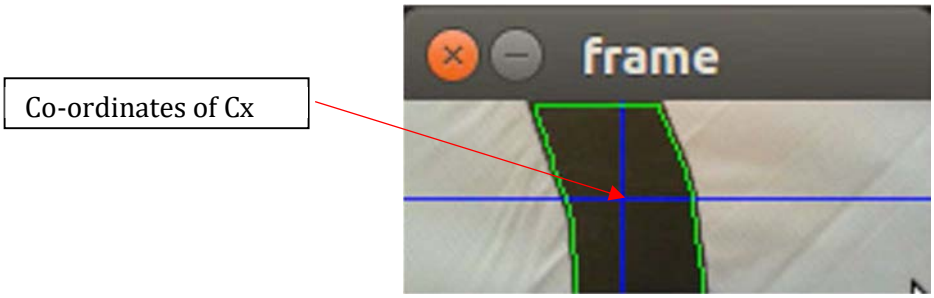

Fig. 28 Centroid of Contour area Cx

The centroid of the contour area is the decision-maker after detection of the line, so according to the value of Cx, the driving decisions of the motors E5 and E6 are made.

In line-tracking, the functionality of the ESC DC motors is very important after the detection of the line of the pipeline. Here, motors E5 and E6 function to track SAUV in the track by actuating simultaneously or separately as per controls command. As thrusters are set in the way that in computer vision algorithm if Cx < 0 then the SAUV lost and continues to perform feature matching in consecutive image frames. While Cx <0, then according to the values of Cx the E5 and E6 motors are actuated. For Cx>= 150, E5 then E5 motor (left side motor) starts to actuated and continues until the SAUV finds line features. While 0< Cx <=40, the E6 motor (Right side) starts to actuated and continues until the SAUV finds line features. When 40<Cx<150, then both E5 and E6 are on as per the shown mission plan.

4.1.4 Vision-based blob(leakage)Detection

The vision-based blob detection will be performed by SAUV during its tracking along with the pipeline. The detailed procedure has been shown in the following Fig. 29.

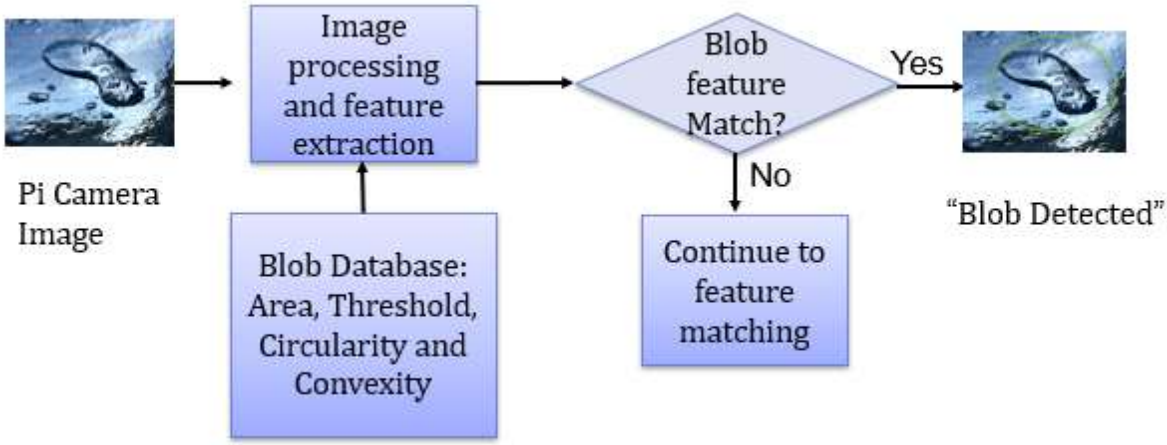

Fig. 29 Vision-based blob detection

In vision-based blob detection, the spillage of gas will create blobs in the underwater environment. During the operation, the Pi camera will capture the instantaneous blob images and those images will pass through image processing and feature extraction techniques such as Canny edge detection. After getting contour validation, Hough Transform will be applied to the contour area. If it matches the pre-indexed database of blob features such as area, threshold, circularity, and convexity, then the message will display as" Blob Detected". If the blob is not detected then SAUV will continue to find feature matching.

As per Fig. 23, Hough Transform (HT) has been known as a very powerful tool for recognizing parametric curves in images. This is implemented through a voting procedure that multiplies the image edge points by multiplying the correctly defined parameters.

Circular Hough Transform (CHT) is a modified version of HT. The purpose of using CHT is to detect circular patterns in the image view. CHT is used to convert a set of feature points in an image space into a set of votes stored in the parameter space. Then, for each feature point, the votes for the combination of all the parameters are collected in the accumulator array. The array element which includes the highest number of votes indicates the presence of a statistic. The pattern of the circle is denoted by (1) where x0 and y0 are the center points and r are the radius of the circle.

However, the threshold is the most frequently changing parameter in blob detection during this operation because the underwater environment has some limitations in lightning conditions. The other variable parameters of the blob are radius, coordinates, and shape.

4.1.5 SAUV Balancing

As shown in Fig. 30, the SAUV is in manual mode at the start, and it is manually operated at the start by joystick and umbilical cable. After switching the operation in auto mode, the MPU 6050 sensor module continuously checks the balancing position in terms of the angle setup value. If the real-time angle value is equal to the set value, then SAUV is in a balanced position and it will continue to check the parameters. While the real-time angle value is less or greater than the pre-set value, then the four motors M1, M2, M3, and M4 will be actuated to balance the SAUV.

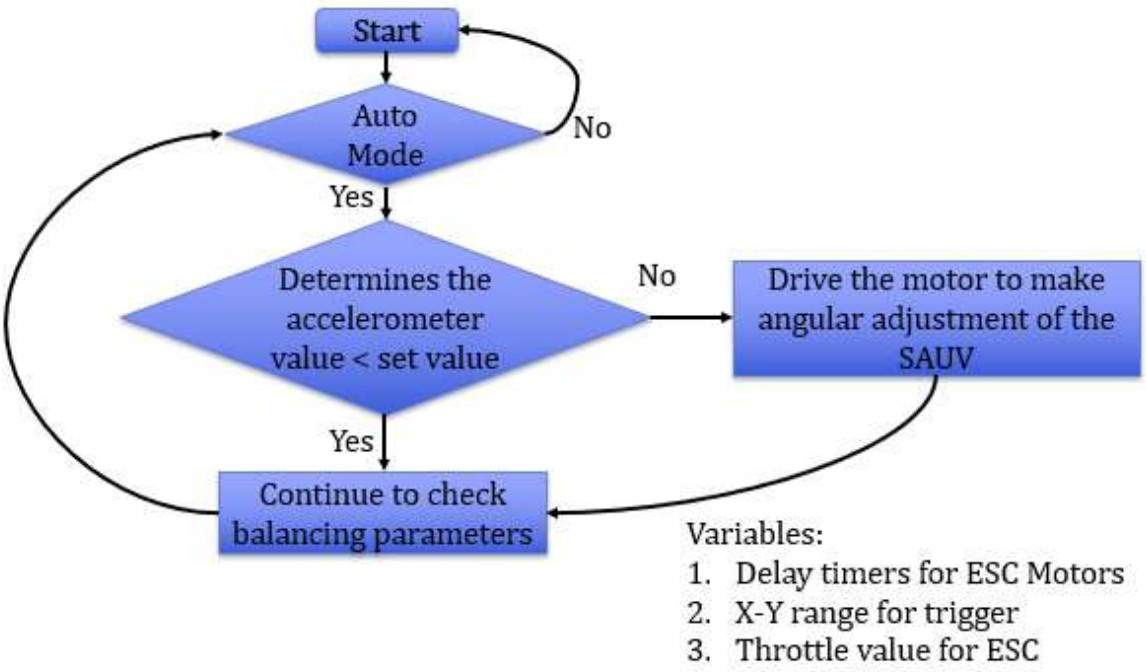

Fig. 30 SAUV balancing

The balancing of the SAUV will be done in +X and -X, +Y, and -Y positions. The controller sends a command to actuate motors depending on their unbalance in the X and Y-axis positions. The controller also gets feedback signals of the balancing.

It is important to mention here that, the ESC motors are powered up by a 12 V battery supply which is installed inside the SAUV capsule. In balancing we only use the accelerometer data in X and Y axis i. e. Ax and Ay of MPU 6050 in the balancing conditions. The raw data of Ax and Ay are normalized and gravity factor is taken into account to get scale data of the accelerometer.

Acceleration along the X axis = (Accelerometer X axis raw data/16384) g.

For example, after 2' complement we get accelerometer X axis raw value = +15454

Then Ax = +15454/16384 = 0.94 g.

The drifting deviation during the operation can be eliminated by using a low pass filter in the circuit. To make the whole operation smooth, the threshold value of the motors is chosen in such a way, that SAUV balanced itself smoothly and don not get any jerk or shock during balancing.

4.2 Conclusion

The SAUV design, architecture, required building materials, vision-based algorithms for balancing have been discussed here for a better understanding of the SAUV concept and its functionality based on the vision system. The experiments will be performed on this basis in the next chapter.

CHAPTER 5

DEVELOPMENT AND TEST RESULTS

5.1 Overview

In this chapter, we will discuss the development procedure and test results of the proposed SAUV approach and its functionality of submarine pipeline detection using a vision-based method. The SAUV functionality in different situations such as lighting conditions, turbulence in the water, and detection of various sizes of blobs in blurry water will be evaluated through different experiments and tests on SAUV.

Here, a SAUV has been tested for balancing in the underwater environment, switching operations in manual/ auto mode, tracking along with the pipeline, and blob detection. Also, the performance of the SAUV in each condition and setup has been evaluated and the changes are made to perform the operation prompt and smooth has been also discussed. The conditions in which the SAUV performance is limited is also shown.

5.2 SAUV performance in Manual/Auto mode

The proposed model of SAUV has been designed in such a way that it can be operated in both auto and manual mode as per requirement.

In below Fig. 31, it can be seen that a push button has been placed in the controller unit to switch the SAUV operation from manual to auto mode. Here a joystick and umbilical cable is connected to the SAUV to transmit the control signal in manual mode.

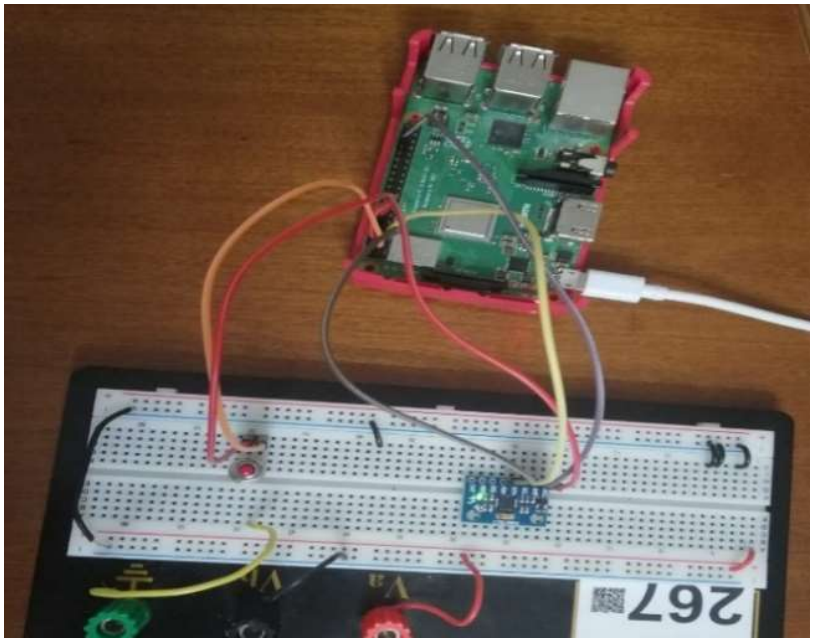

Fig. 31 Experimental Set-up of Auto/Manual Mode: SAUV

At the beginning of the operation, the SAUV has been controlled by a joystick and umbilical cable until it gets balanced over the line in underwater. After balancing the joystick sends a signal to the SAUV controller to switch on auto mode. After getting the signal, a SAUV starts balancing itself and continues to drive underwater.

```
        if accel_data['x'] > 2:
            SERVO = 4
            pi = pigpio.pi() # Connect to local Pi.
            pi.set_servo_pulsewidth(SERVO, 501) # Minimum throttle.
            time.sleep(0.5)
            pi.set_servo_pulsewidth(SERVO, 1500) # Maximum throttle.
            time.sleep(0.5)
            pi.set_servo_pulsewidth(SERVO, 550) # Slightly open throttle.
            time.sleep(0.5)
            pi.set_servo_pulsewidth(SERVO, 0) # Stop servo pulses.
            pi.stop()
        else:
            print("BALANCED")
    else:
        print("MANUAL MODE ACTIVE")
```

5.3 SAUV Balancing

SAUV balancing has been performed by the simultaneous operation of the MPU6050 sensor module and DC Motors through the controller in the mission plan.

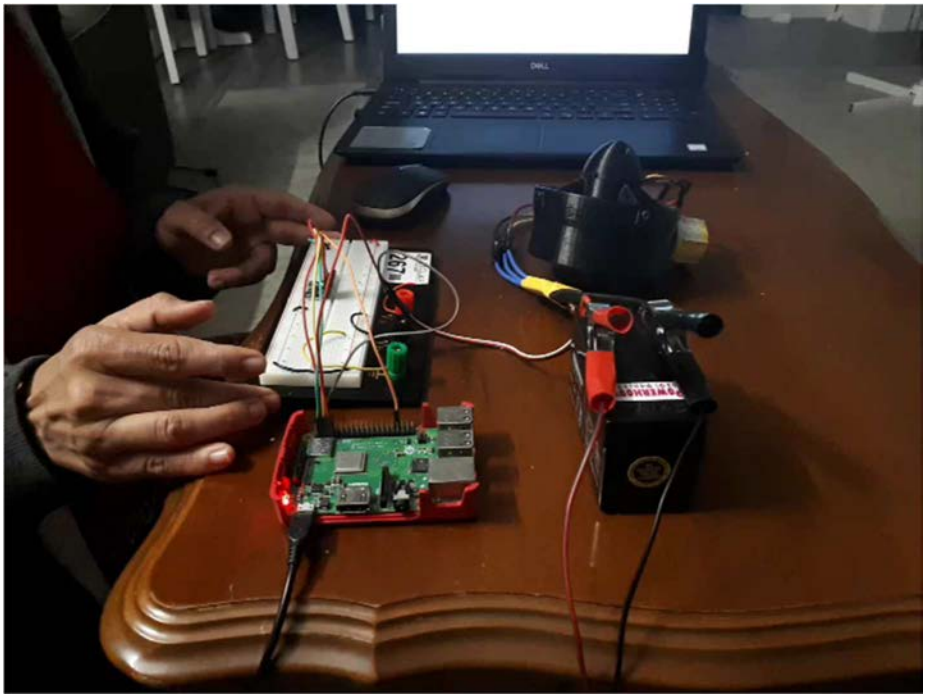

Fig. 32 Experimental Set-up of SAUV balancing

In Fig. 32, the experimental setup of the controller unit with all inputs and outputs has been shown. Here, The MPU 6050 sensor module has been used as a sensor for tracking the balancing condition of the SAUV. The accelerometer data of the MPU6050 has been used here to define and correct the position of SAUV. The raw accelerometer data has been scaled in terms of g and as per input accelerometer data, the controller will command DC motors for actuation. Here there are for DC motors M1, M2, M3, and M4 are positioned as per in Fig. 32. The experiment was carried out in three steps to check their functionality in different possibilities of tilting and analyze their thrust measurement.

Step 1: The motors M1 and M2 are considered for balancing in +X and -X position

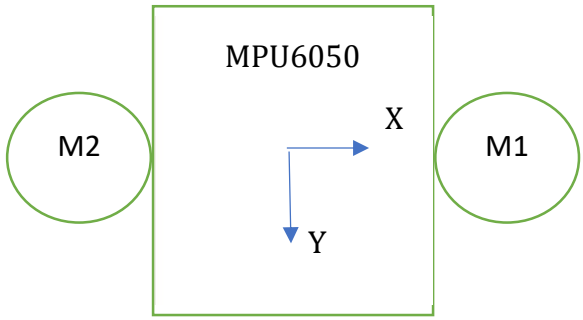

Fig. 33 MPU6050 with Motors M1 and M2

As per the experiment setup in Fig. 33, in balance condition, M1 and M2 both are on. If the value of X >2, then M1 stops to actuate, and M2 changes its thrust value to balance the SAUV to get the preset value of X. The preset value of X is defined as +2. Conversely, if the value of X <2, then M2 stops and M1 starts to change its thrust to get the balanced position.

Step 2: The motors M2 and M3 are considered for balancing in +Y and -Y position

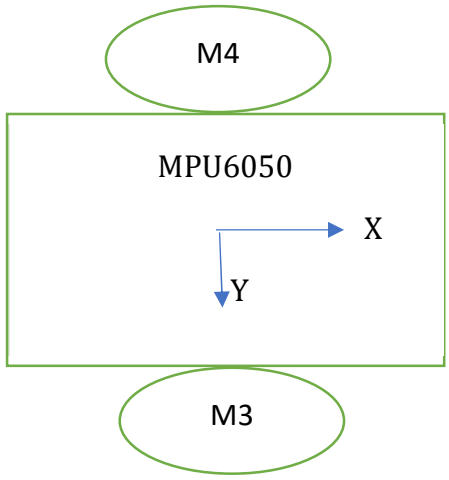

Fig. 34 MPU6050 with Motors M3 and M4

A per experiment setup in Fig. 34, in balance condition, M3 and M4 both are on. If the value of Y>2, then M3 stops to actuate, and M4 changes its thrust value to balance the SAUV to get

the preset value of Y. The preset value of Y is defined as +2. Conversely, if the value of Y <2, M4 stops and M3 starts to actuate in the speed to get the balanced position.

Step 3: The motors M2, M3 set and M1, M4 set are considered for balancing in +X and -X position and M2, M3 set and M1, M4 set are considered to balance in +Y and -Y Axis.

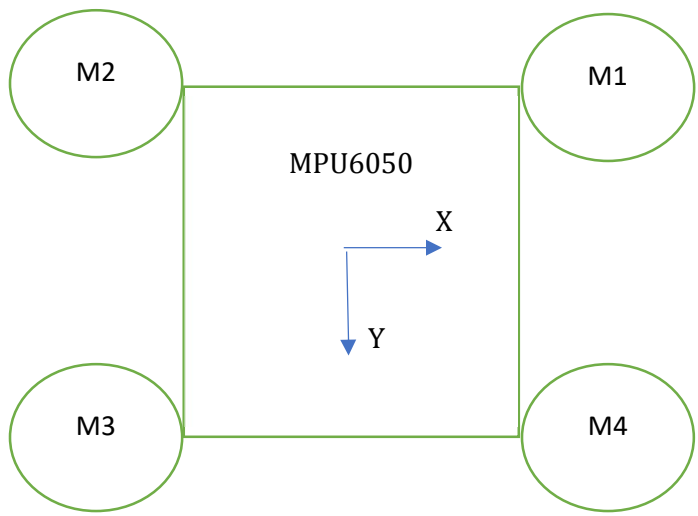

Fig. 35 MPU6050 with Motors M1, M2, M3 and M4 Motors

A per experiment setup in Fig. 35, in balance condition, M1, M2, M3, and M4 are on. While unbalance occurs in +X position i.e., SAUV gets in unbalanced position +X – Axis and the value of X > 2, then M2 and M3 start to actuate to make the value of X = 2, and if X < 2 then M1 and M4 start to actuate with the maximum thruster. For the other possibility, if the unbalanced condition persists in Y-axis and Y >2, M3 and M4 start to actuate to make the balance, and if Y < 2 M2 and M3 start to actuate.

If the value of Y>2, then M2 stops to actuate, and M3 changes its thrust value to balance the SAUV to get the preset value of Y. The preset value of Y is defined as +2. Conversely, if the value of Y <2, M2 stops, and M3 start to actuate in the speed to get the balanced position.

As discussed, all the conditions in Steps 1,2, and 3 the according to the experiment, the ESC motors are started to actuate as per the defined condition. The test positions them are shown in Fig 36.

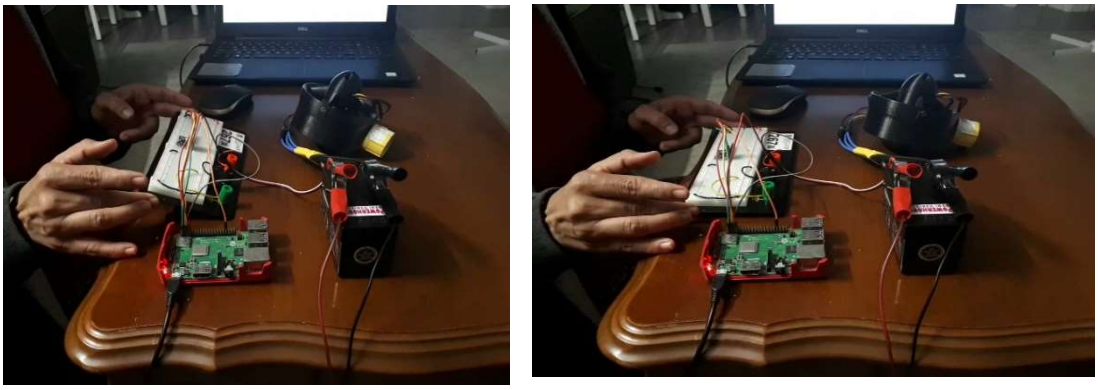

Fig. 36 Tilted position and steady position of MPU6050 with ESC DC Motor

Table 2: Drifting Deviation and RMSE on static position of MPU 6050 sensor

	X- Axis		Y- Axis	
	Drift 5 min	RMSE	Drift 5 min	RMSE
σ_{gyro}	22.84°	1.3e-4	45.15°	1.4e-4

Table 3: Drifting Deviation and RMSE on movement position of MPU 6050 sensor

	X- Axis		Y- Axis	
	Drift 30Sec	RMSE	Drift 30 Sec	RMSE
σ_{gyro}	48.41°	24.11°	4.38°	11.35°

After achieving the feedback of the MPU 6050 sensor module in both static and movement positions, it is also important to measure thrust to decide the motor speed according to the sensor data. The thrust value of the BLDC motor which is measured through the experiment is shown in Fig. 37:

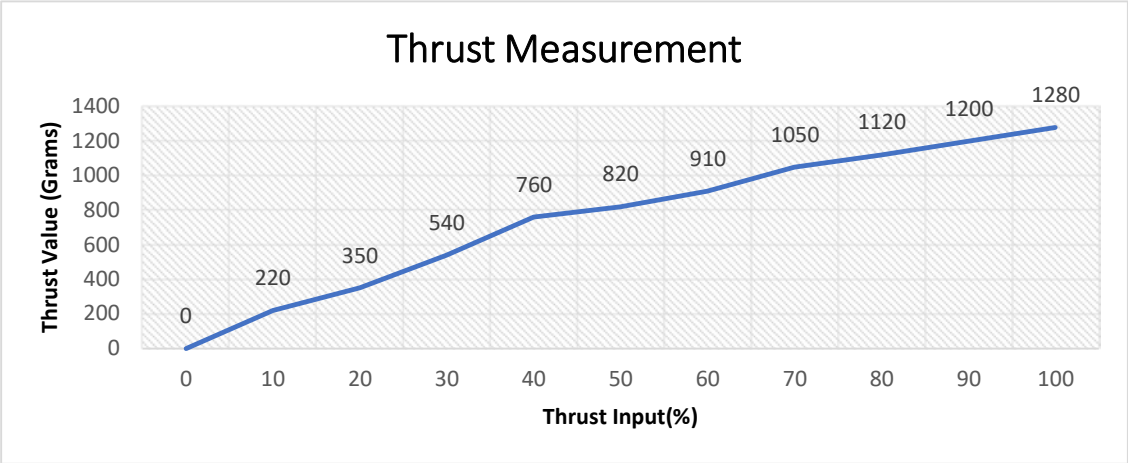

Fig. 37 Thrust Measurement during experiment

In conclusion, we have performed experiments in steps to test the balancing in X and Y directions through the MPU6050 sensor and four motors. After testing the DC motor thrust and sensor feedback, we were able to decide the speed of the motor for balancing operation smoothly.

5.3.1 Influence of turbulence of water in balancing

For the experiment, the water is assumed to be still and clean, but the actual experiment was carried out to test the performance of the SAUV in minimal turbulence conditions. The experiment result was different than it was calculated before. The DC Motor's response took more time it was expected, so the response time was more as compared to the calculated time. In addition, it required more thrust in this condition as compared to the normal condition.

Estimated Orientation from -90 to +90 degrees(X-axis)

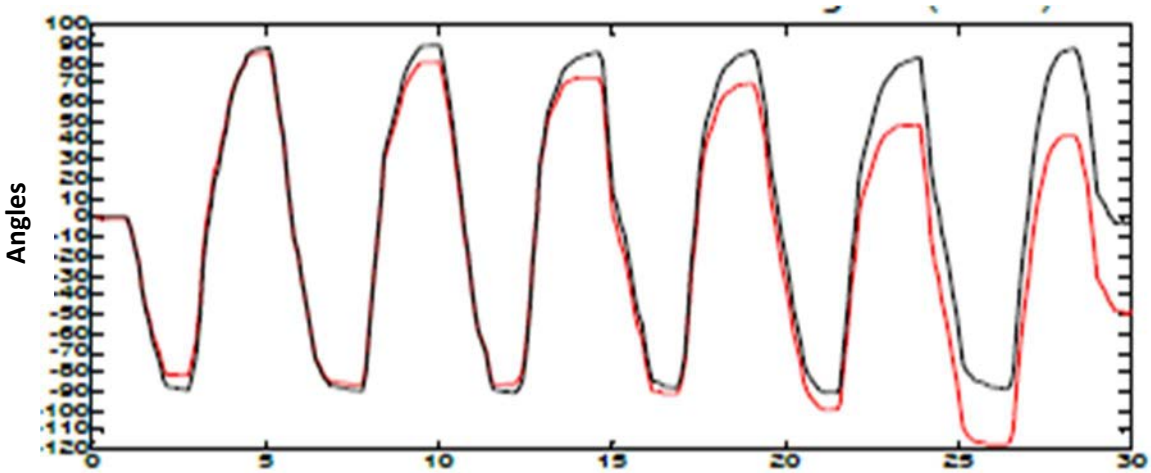

Estimated Orientation from -90 to +90 degrees(Y-axis)

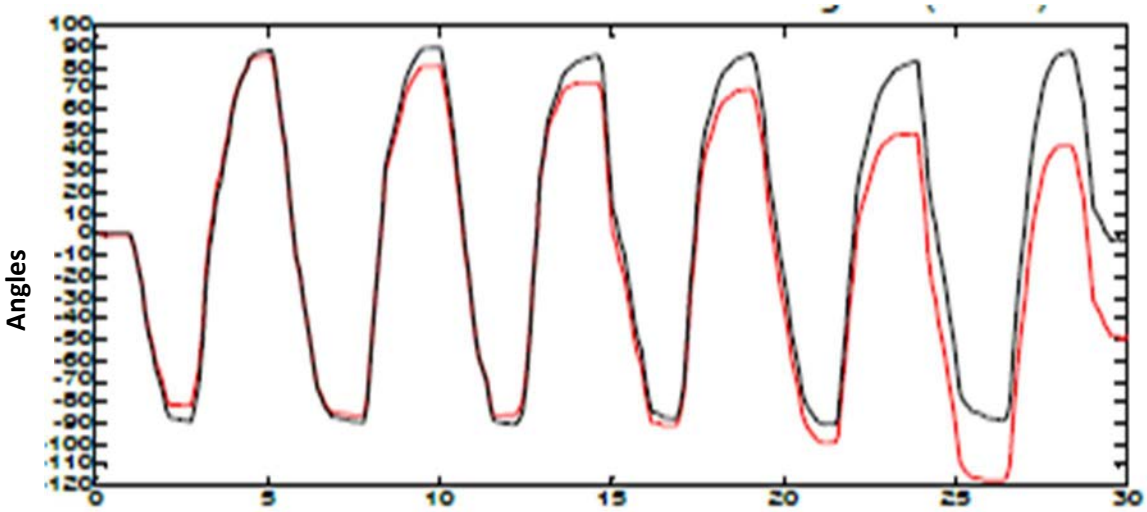

Fig. 38 Analysis of SAUV Balancing in -90 to +90 degrees [14]

5.4 Vision-based SAUV Tracking

SAUV balancing has been performed by a vision-based algorithm to track the SAUV along with the pipeline.

For experimental setup, the Pi camera has been placed in an assembly to track SAUV by a vision -based algorithm in order to test tracking of the SAUV along with the pipeline and two DC motors have been placed on each left and right side to keep it on tracking.

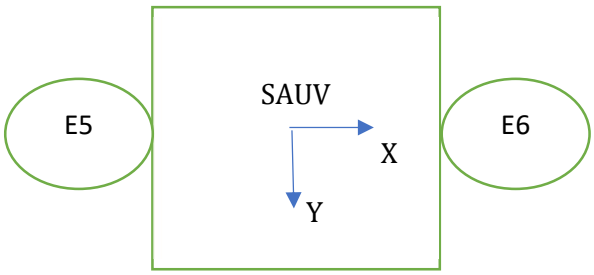

Fig. 39 Arrangement of motors for Line Tacking

As shown in Fig. 39, two DC motors E5 and E6 are positioned on the left and right side respectively to keep the SAUV on line track. The control value Cx (centroid of X) for actuation and thrust of the motors have been decided as per image frame pixels and line parameters. As per the controller programming for line tracking, if Cx >= 150 then E5(left side motor) starts actuating, and while 0<Cx<40, E6 motor starts actuating. Here, in an actual experiment, both motors are on when the Pi camera is on the line. In the on-track situation, both E5 and E6 are off. While we move the Pi camera assembly on the left side of the drawn line, then E6 motors get high thrust to move the object on the right side i.e., on the line track. While the move this assembly on the right side of the said line, then E5 starts to actuate at high thrust to move the object on the left side. In the situation, while Cx<0, then SAUV is considered as a lost and continues looking for a feature matching of the line.

Presently, the Pi camera has been placed in one assembly, Raspberry Pi and motors and other setup have been situated outside the SAUV enclosure, but in actual application, Raspberry Pi board and the Pi camera will be placed in the waterproof console inside the body of SAUV.

Here for ease of execution of the programming, we have drawn the black line on the paper, but in an actual application, we will draw a white line at the bottom center of the pipeline so it can be more visible in dark and nighttime in the underwater environment.

```
if cx >= 150:
    SERVO1 = 12
    pi = pigpio.pi() # Connect to local Pi.
    pi.set_servo_pulsewidth(SERVO1, 1100) # Minimum throttle.
    time.sleep(5)

if cx < 100 and cx > 40:
    SERVO1 = 12
    SERVO2 = 21
    pi = pigpio.pi() # Connect to local Pi.
    pi.set_servo_pulsewidth(SERVO1, 1100) # Minimum throttle.
    pi.set_servo_pulsewidth(SERVO2, 1100) # Minimum throttle.
    time.sleep(5)

if cx <= 40:
    SERVO2 = 21
    pi = pigpio.pi() # Connect to local Pi.
    pi.set_servo_pulsewidth(SERVO2, 1100) # Minimum throttle.
    time.sleep(5)
```

The test results of implementation of above algorithm are as shown in Fig. 40

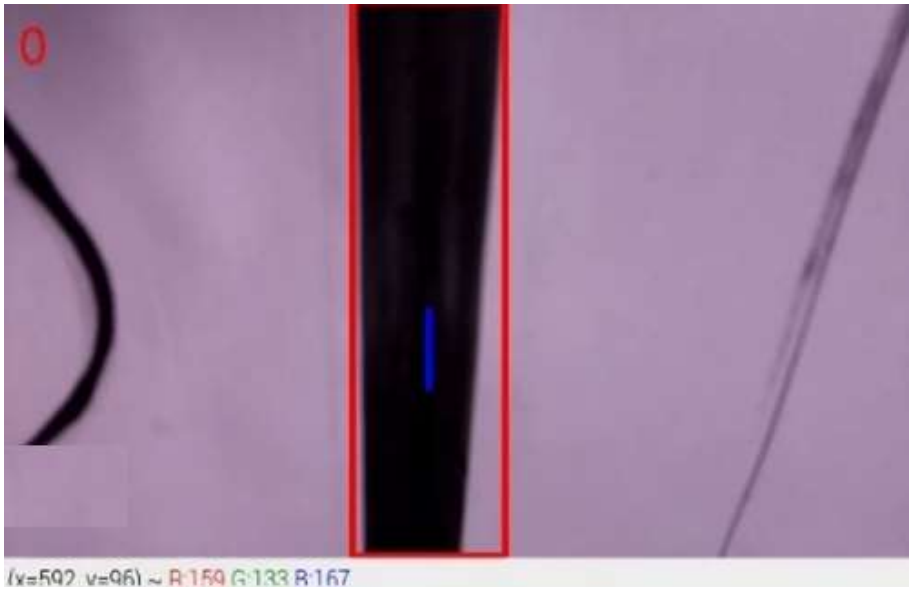

Fig. 40 Test results for Line Tracking

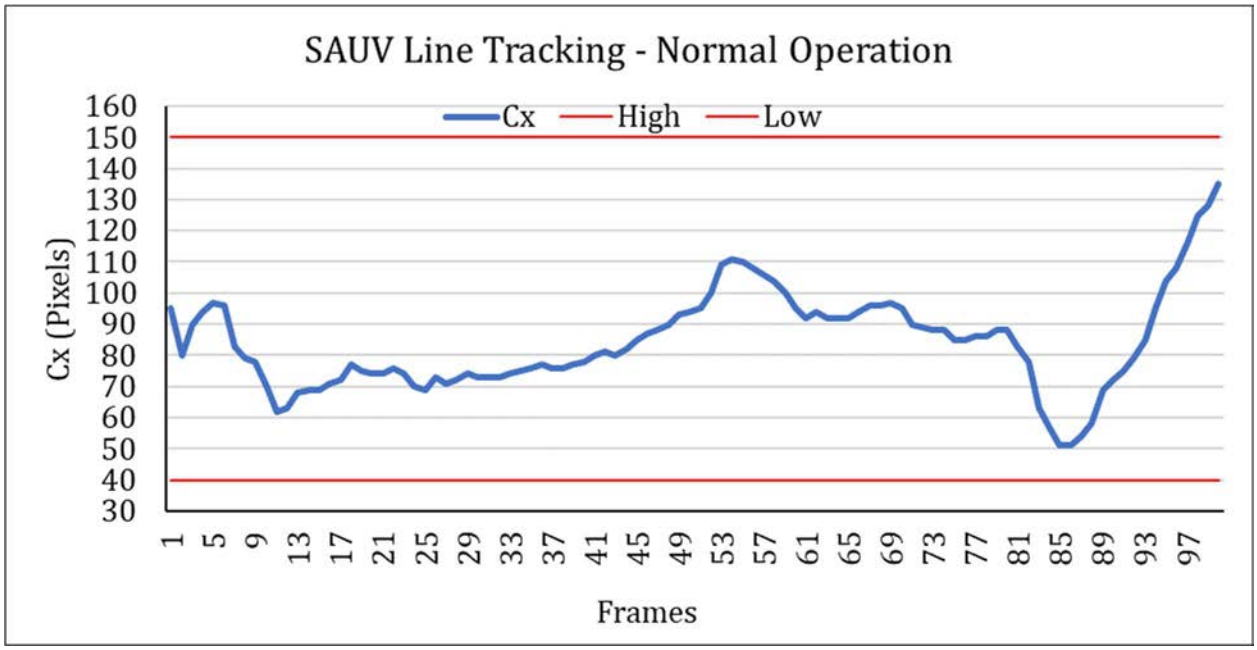

Fig. 41 Graphical Representation of Test results for Line Tracking

In Fig 41, the "Up Limit" and "Lo Limit" are the trigger points to increase the threshold value of the ESC motor to maintain the direction of SAUV along with the line. The graph shows that the fluctuation of Cx value slightly and within the stipulated range. In this scenario, both the ESC motors will run at the same speed. During the simulation frame rate is set at 20 instances per second, so that camera is taking 20 results per second to achieve higher accuracy.

5.4.1 Influence of Turbulence on SAUV Line Tracking

In the experiment of getting results and determine the influence of turbulence on the Line Tracking, artificial turbulence was generated and results of Cx values were taken. The simulation result is shown in Fig 42 and the graphical representation of recorded Cx values is shown in Fig 43. In this result Camera is still finding proper values of Cx even with the

variation of Line thickness due to turbulence because the algorithm derives the centroid of Line to calculate Cx with the higher framerate.

Fig 42 Test result of Line tracking with Turbulence

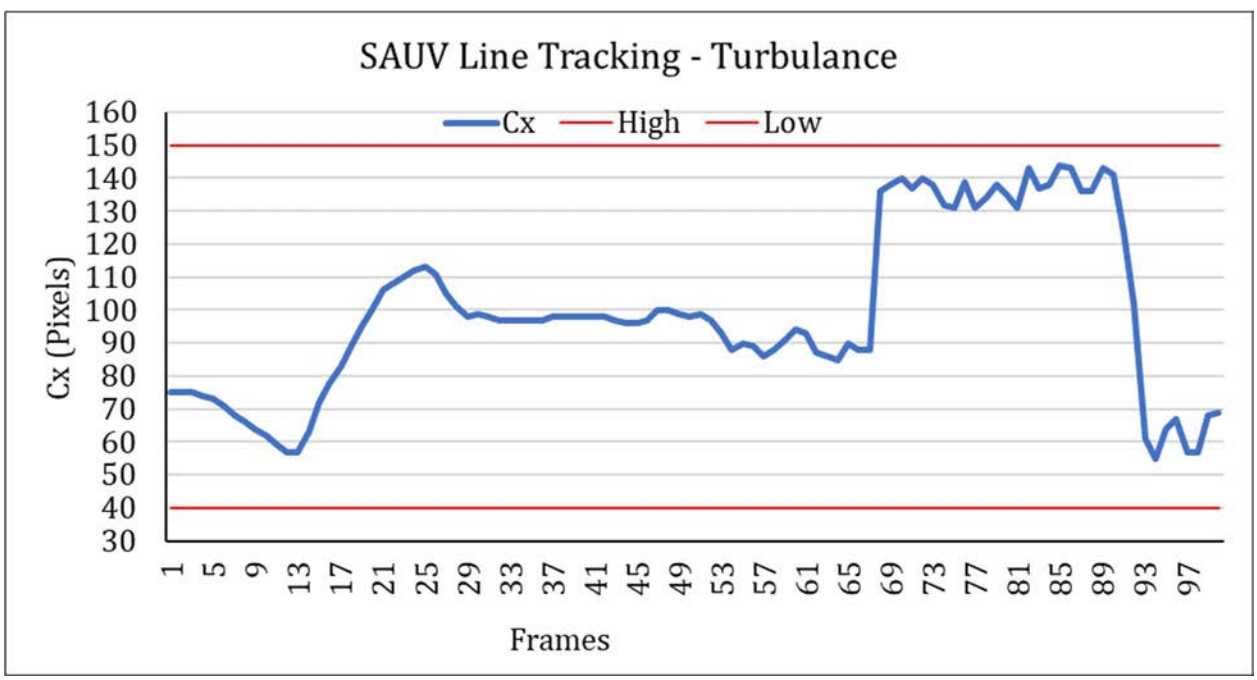

Fig 43 Graphical Representation of Test results for Line Tracking with Turbulence

5.4.2 Influence of Lighting Conditions on SAUV

Presently, the experiment is carried out in both day and night light conditions. According to the test, the Pi camera and both motors function as per the predefined condition of the line tracking algorithm, but in dark time it needs to adjust a little bit threshold value for better contrast in the vision algorithm. However, the Pi camera that we are using here is a NoIR (Non-infrared) camera so it performs very well as compared to a normal camera. Fig. 44 is shown the test simulation with very low lighting. In this scenario, even the NoIR camera is not getting adequate contrast to derive Cx value, and it is considering the mid-point of the field of view (FOV) which is 95.

Fig. 44 Test Result with Low Lighting

The lighting limitations can be eliminated by mounting the LED light on the SAUV enclosure on the top at the front side for better results. Fig 45 is shown the simulation result of line tracking in the dark environment with add-on fixed lighting on SAUV.

This arrangement has been tested with LED lighting ON/OFF scenario and recorded the Cx values, which graphical representation is shown in Fig 46.

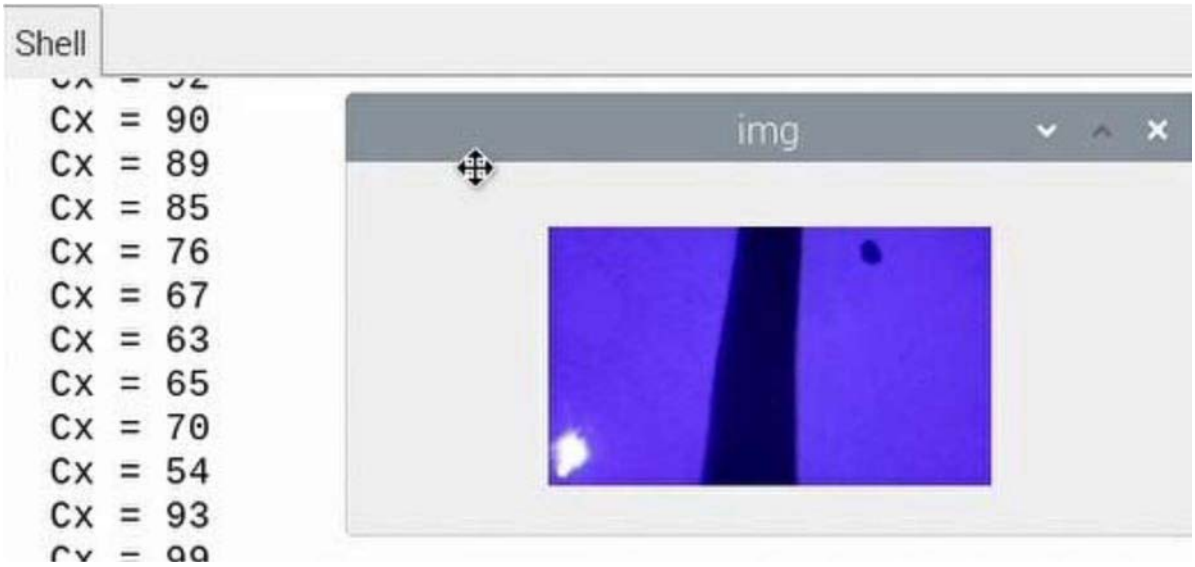

Fig 45 Test result of Line Tracking in the Dark with Add-On Lighting

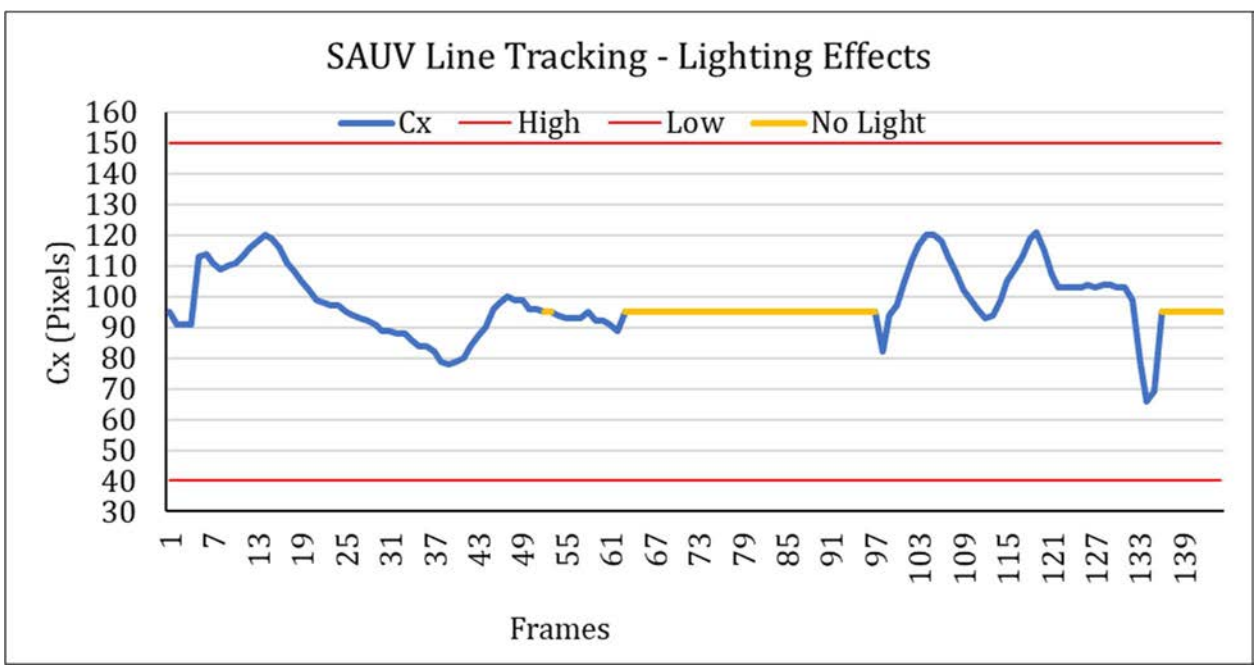

Fig 46 Graphical Representation of Line Tracking in Dark with Add-On Lighting

In addition, with the current setup of add-on lighting in the dark environment, the turbulence has been added and a test has been performed to record the test results. The Simulation result of the test is shown in Fig 47.

Fig 47 Test result of Line Tracking in the Dark with Add-On Lighting and Turbulence

5.4.3 Influence of Irregular Line on SAUV Line Tracking

The test has been performed for irregular line tracking by SAUV, and simulation results recorded as shown in Fig 48.

The test results show that the irregular line within the field of view did not affect the performance of line tracking while SAUV travels along with the line so that the centroid of the irregular line will be within the field of view of the Camera. Whenever the line goes beyond the field of view, far-right or far-left, the threshold value of the ESC motor will increase and SAUV will again along with the line and centroid of the line will be within the field of view.

Fig 48 Test result of Irregular Line Tracking

The lighting effects on the line tracking with a straight line and irregular line will impact a similar way, but turbulence will impact differently on irregular line. The test has been performed for irregular line tracking during the turbulence and results of Cx have been recorded. The simulation result of irregular line tracking with turbulence is shown in Fig 49 and graphical representation is shown in Fig 50. During the turbulence, the Cx value fluctuates momentarily which is inaccurate and it happens due to false reflection of line in turbulence. This false and momentarily fluctuation can be eliminated through an algorithmic filter. The graphical representation of the test result with filter is shown in Fig 51.

Fig 49 Test result of Irregular Line Tracking with Turbulence

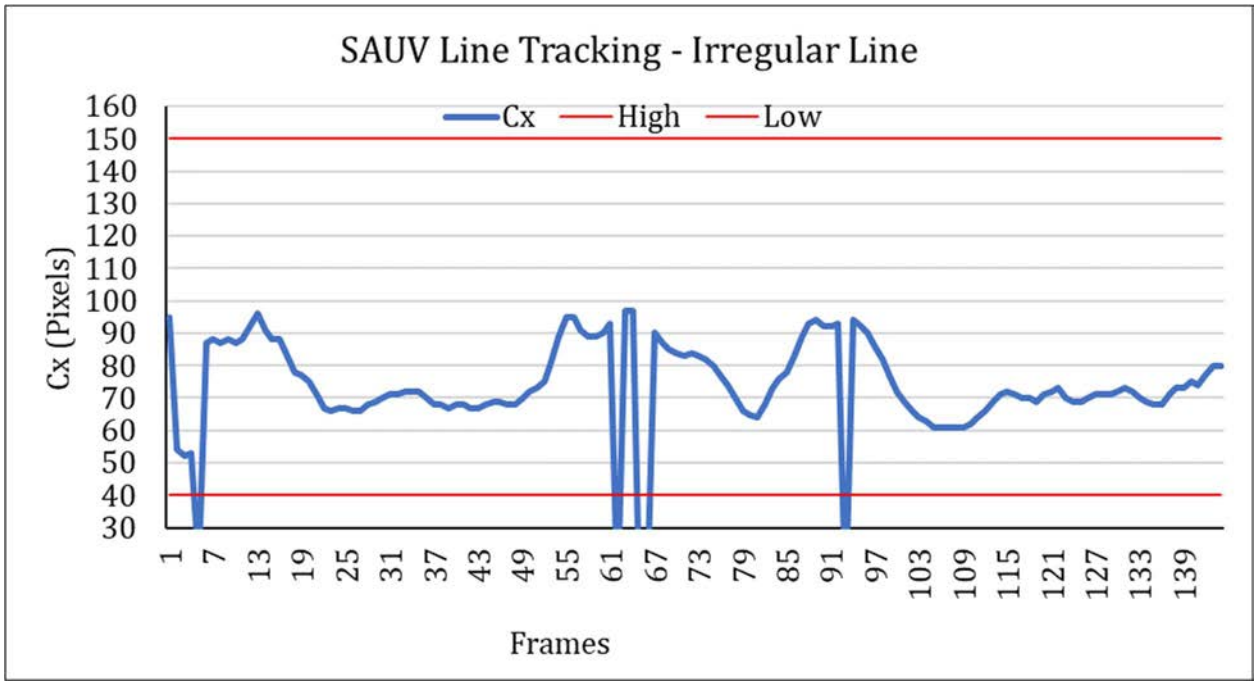

Fig 50 Graphical representation of Irregular Line Tracking without Filter

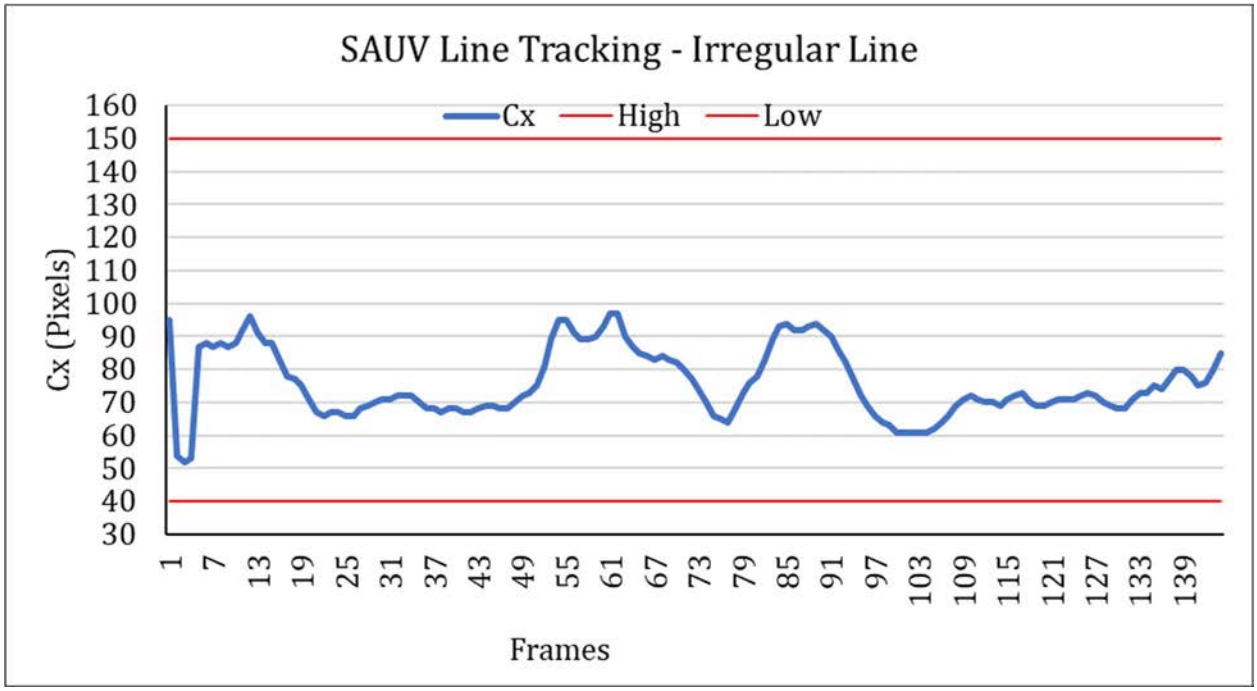

Fig 51 Graphical representation of Irregular Line Tracking with Filter

5.5 Vision-based spillage Detection by SAUV

Vision-based spillage detection has been performed here by recognition of blob created by a gas pipeline in the underwater environment. The blob detection through computer vision algorithm has been tested here through an experiment.

Fig. 52 Experimental Set-up for blob detection

As shown in Fig. 52, blob detection has been performed by placing a whole controller assembly in the SAUV enclosure. The bubbles have been created in water and the SAUV capsule has been put into the water in a small vessel. The Pi camera captures bubbles of all sizes in the water and provides a feedback signal as “blob detected” on the screen.

Fig. 53 Test Result of Blob Detection

As shown in Fig 53, SAUV detects blobs that have been created during operation by pipeline leakage. The size of the detected bubbles varied from the area of 800 pixels to 1800 pixels and SAUV has been successful to capture the leakage bubbles of this range or limit.

5.5.1 Influence of Blob Size in Spillage Detection

During the experiment, various sizes of blobs are created in the water to test the ability of SAUV for recognizing the blob in the water. The contrast and threshold values have been set up in the vision algorithm to maximize the capacity of blob detection in both day and night time.

As shown in Fig 54 and Fig 55, SAUV can only detect the bubbles which are in the predefined limit of area in pixels through green circles, and undetected bubbles are in “red circles”. SAUV is unable to consider the bubbles which are not within the stipulated limit. However, while the large bubble comes to a smaller size within the limit, SAUV is able to detect it. In Fig 55, the graphical representation is shown the total bubbles in the field of view and detected bubbles over the time

of record of test results. In this experiment, the framerate is 10 instances per second to achieve a better result.

Fig. 54 Influence of blob sizes in spillage detection

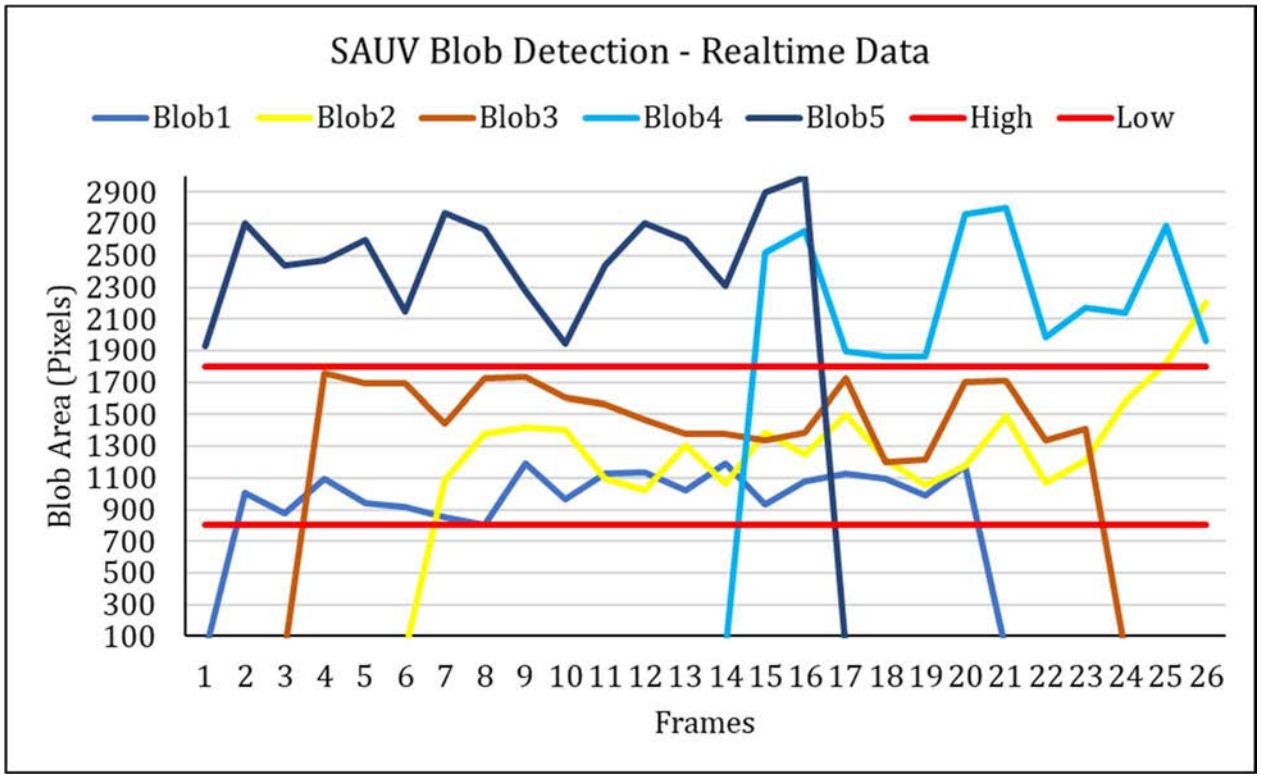

Fig. 55 Graphical Representation of influence of blob sizes in spillage detection

Table 4: Recorded Results of Area in pixels for Blob Detection Experiment

Frame	Blob1	Blob2	Blob3	Blob4	Blob5	UL	LL
1	0	0	0	0	1931	1800	800
2	1010	0	0	0	2706	1800	800
3	880	0	0	0	2435	1800	800
4	1093	0	1761	0	2471	1800	800
5	942	0	1697	0	2602	1800	800
6	920	0	1697	0	2149	1800	800
7	851	1083	1439	0	2771	1800	800
8	807	1377	1723	0	2665	1800	800
9	1196	1415	1734	0	2277	1800	800
10	967	1401	1601	0	1945	1800	800
11	1129	1099	1566	0	2436	1800	800
12	1133	1020	1464	0	2702	1800	800
13	1019	1306	1382	0	2596	1800	800
14	1190	1059	1377	0	2309	1800	800
15	930	1384	1340	2520	2900	1800	800
16	1079	1252	1390	2660	3000	1800	800
17	1131	1496	1726	1899	0	1800	800
18	1094	1214	1202	1863	0	1800	800
19	991	1052	1216	1865	0	1800	800
20	1176	1179	1700	2760	0	1800	800
21	0	1495	1706	2800	0	1800	800
22	0	1073	1337	1985	0	1800	800
23	0	1207	1413	2171	0	1800	800
24	0	1580	0	2142	0	1800	800
25	0	1820	0	2692	0	1800	800
26	0	2200	0	1959	0	1800	800

The recorded values of the area of blobs in pixels are represented in Table 4, where the frame is the instance of captured values of different blobs within the field of view.

5.5.2 Blob (Spillage) Detection Accuracy

The process of creation of bubble, variation of size, and disappearance of it is continuous and rapid. In Fig 56 is a comparison between expected numbers of blob and detected numbers of the blob to determine the accuracy of blob detection during the test record.

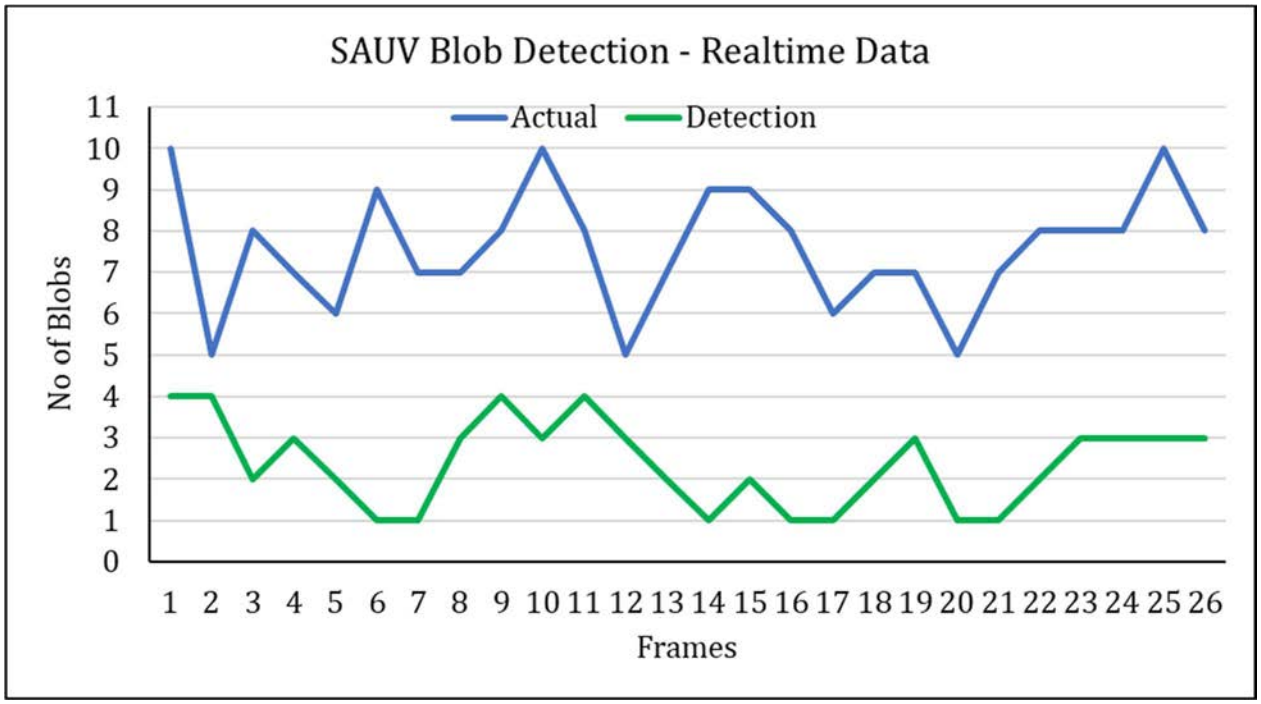

Fig. 56 Graphical Representation of Blob Detection Comparison in Normal Operation

As discussed earlier, SAUV detects blobs that are in between 800 to 1800 pixels as per the defined algorithm. During experimental operation, we get the accuracy varies between 0.5 to 0.98 as shown in Fig. 57. If we generate turbulence in the water, it affects the accuracy of SAUV. In turbulence, as shown in Fig. 58, accuracy decreases as compared to the normal operation. The SAUV fails to differentiate the blobs created by spillage detection and blobs of turbulent water.

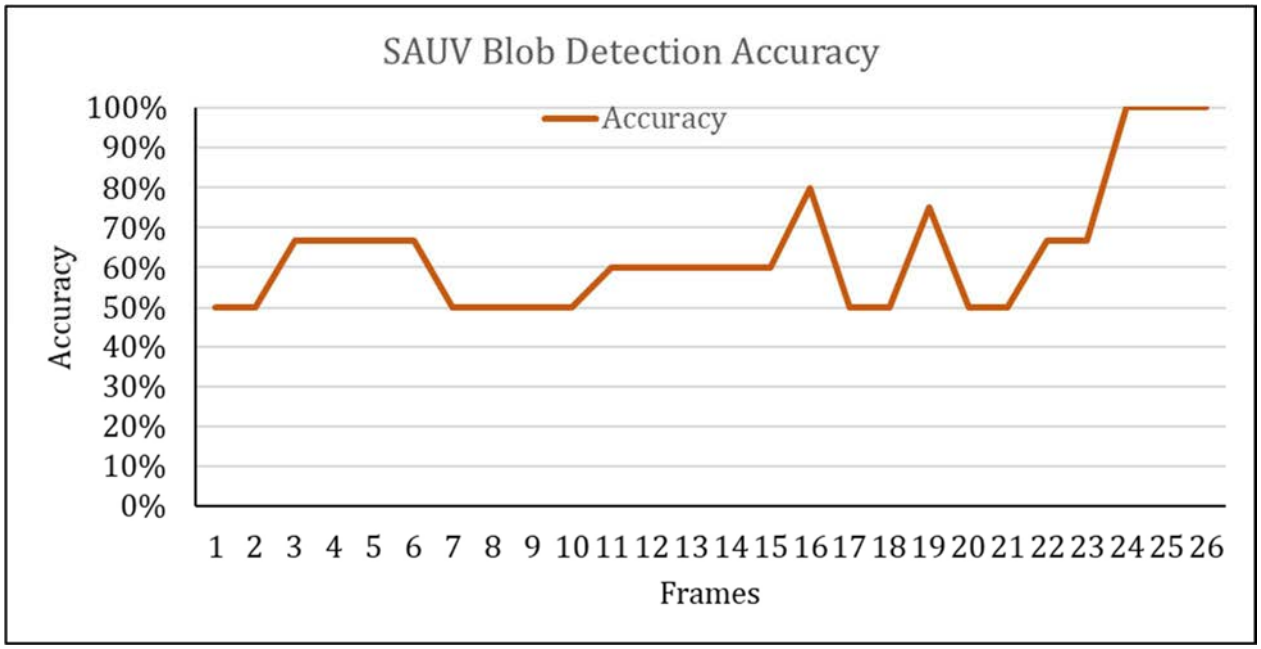

Fig. 57 Graphical Representation of Blob Detection Accuracy in Normal Operation

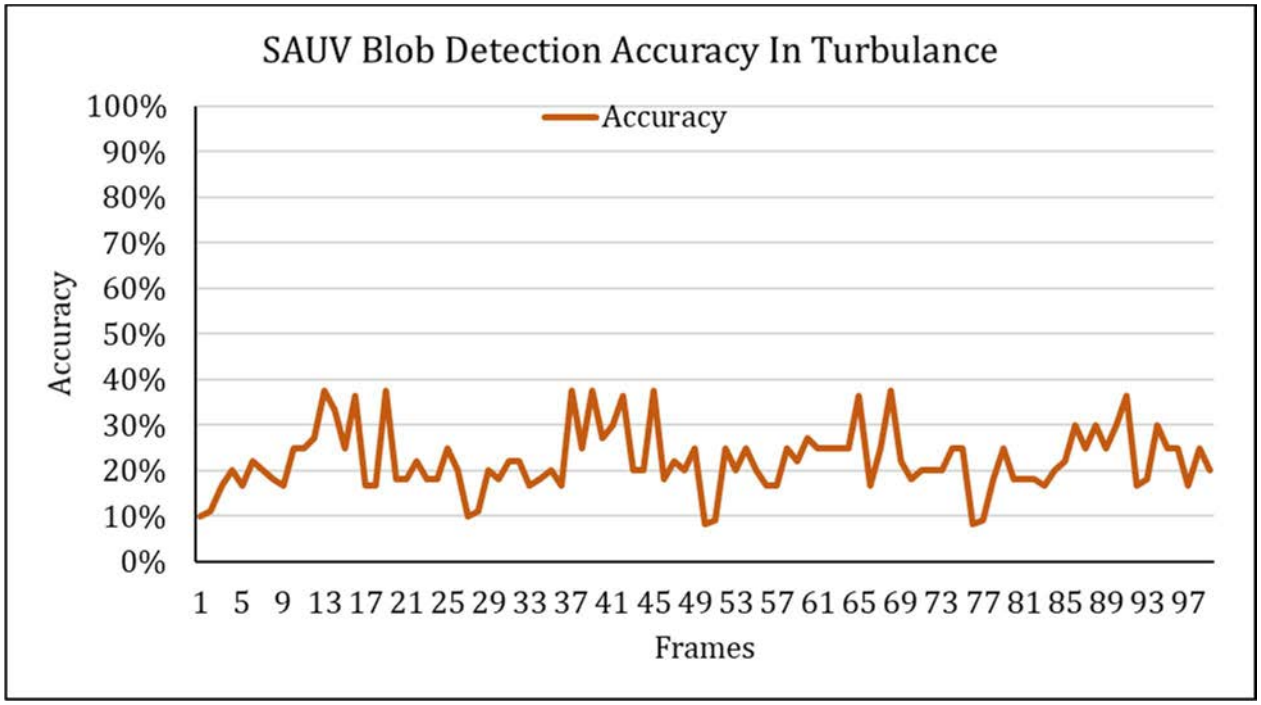

Fig. 58 Graphical Representation of Blob Detection Accuracy in Turbulence

5.6 Challenges and Limitations

During testing the SAUV in different conditions of the underwater environment, the performance analysis is as below:

Fig. 59 Before (Left) and After (Right) Arrangement of DC Motors for SAUV Balancing

In Fig. 59 the arrangement of four DC Motors shown with a different position referencing SAUV. In the left side arrangement, the M1, M2, M3, and M4 are placed on the middle of the four sides of SAUV. In this condition, the SAUV can tilt in eight ways underwater while driving. On the other way, according to the right-side arrangement of the motors, the four possibilities of tilting can be avoided by the positioning of DC motors in each corner of the SAUV. So, in this arrangement, the SAUV will unbalance in four sides up and down, and it can balance itself in each corner. The pulse width module (PWM) is of the four motors is set here to make the operation smooth.

Also, as per the proposed SAUV balancing algorithm, the deviation error which causes the difference between theoretical and realistic angle values can be eliminated by using a low pass filter in the controller circuit. It also reduces the noise level in both static and movement position.

Additionally, through the accelerometer data of the MPU 6050 sensor module, the orientation of the SAUV can only be estimated in the X and Y-axis only. However, as we discussed earlier, the possibilities of maintaining SAUV in the Z-axis in minor due to its arrangement of motors in the middle of each side of the SAUV.

This SAUV has been proposed to perform operations in the water tank. According to the experimental test results, the influence of the light conditions has been discussed before. Also, the turbulence in water is assumed here will affect the SAUV. There is a possibility of SAUV getting away from the track or lost the track in the high underwater currents due to its lightweight. Additionally, for underwater image analysis high transmission attenuation. Molecular scattering, particle scattering, and absorption cause degradation of underwater images. Because of light scattering, the Intensity of plane light I, passing through a medium decrease as per below:

$$I = I_0 e^{-(\mu+h)r} \quad \text{.....(10)}$$

Where I_0 = intensity of incident wave, h = extinction coefficient, r = width of the medium, μ = adsorption coefficient. The other concern is the response curve of the camera which causes a difference in the Grayscale images, and it varies in each camera.

5.7 Conclusion

In conclusion, the experimental setup and test results have been discussed so far here. However, the tasks of the mission plan SAUV balancing, SAUV tracking, and blob detection through a vision-based system have been performed as predefined algorithms despite having some challenges in the underwater environment.

CHAPTER 6

CONCLUSION

6.1 Discussion

The SAUV has been introduced here to perform pipeline leakage detection using a vision-based system. The purpose of this SAUV is to make the operation at a lower cost by using advanced technology of computer vision and machine learning. The proposed design of SAUV makes the operation of SAUV more sustainable and balanced in the underwater environment. The Raspberry Pi, Pi camera, and ESC DC motors – hardware and python language-based programming. OpenCV – software is utilized here to execute a computer vision-based algorithm through the Raspberry Pi controller to hardware. The proposed model is called "SAUV" as it can be operated in both auto and manual modes. However, umbilical cable and joystick are used to perform the operation in manual mode and take the control of SAUV in lost situations. For SAUV tracking along with the pipeline and blob detection computer vision algorithm is proposed here to make the tasks accurate and smoother. These two operations-pipeline tracking and blob detection are performed through the vision-based system in which images are taking by the Pi camera and image preprocessing and feature extraction are applied to them to perform line detection and blob detection tasks. However, the underwater environment is challenging and blurry, some limitations of the proposed algorithms have been seen during the experiment, but they can be avoided by making some changes in threshold and contrast in the algorithm.

The novelty of this research is the dual mode of the underwater vehicle and low cost as compared to existing underwater vehicles available in the market. The proposed SAUV is developed for a depth rating of 10 meters which is suitable only for test tank operations. The SAUV is currently developed for specific industrial application of offshore submarine pipeline spillage detection purpose on which most of the countries' economy is dependent.

6.2 Significance

The leaks in the submarine pipeline industries are the major causes of the enormous damage and losses of human and Eco lives. However, the most popular underwater vehicles are available to carry out the leakage detection of the submarine pipeline, but their purchasing cost is very high. The proposed SAUV is designed to order to perform the spillage detection task at a lower cost. The proposed SAUV has been developed with the use of advanced computer vision technology and algorithm to enhance the better performance as a whole.

6.3 Future Work

Presently, the proposed SAUV has been experimented and test results are taken into the defined level of experiment setup which is compatible with the use of spillage detection in the submarine pipeline network. In the next step, it will be tested in further experiments or real applications. It is expected that the limitations in the current scenario can be overcome with an implementation technology of artificial intelligence and high version of camera.

REFERENCES

[1] A. Bhatnagar, “Image Segmentation Using Canny Edge Detection Technique Kirti,” 04-Mar-2017. [Online]. Available: http://www.ijtmr.com/docs/vol4/ma17(2).pdf. [Accessed: 09-Mar-2021].

[2] A. Minato, M.M.A. Joarder, S. Ozawa, M. Kadoya, N. Sugimoto,” Development of a lidar system for measuring methane using a gas correlation method”,1999, Jpn. J. Appl. Phys. 38, pp 6130–6132.

[3] “An Overview of Pipeline Leak Detection Technologies.” [Online]. Available: https://asgmt.com/wp-content/uploads/2018/03/102.pdf. [Accessed: 09-Mar-2021].

[4] B. Kim and S. Yu, "Imaging sonar based real-time underwater object detection utilizing AdaBoost method," 2017 IEEE Underwater Technology (UT), Busan, Korea (South), 2017, pp. 1-5, doi: 10.1109/UT.2017.7890300.

[5] Bie, Qin, Zheng, Yunping, Fu, Min, Song, Xiaojian, “Leakage detection technology of oil and gas transmission pipelines and its development trend”, 2007 Petrol. Eng. Construct.

[6] C.P. Liou, “Pipeline leak detection by impulse response extraction”, 1998. J. Fluids Eng.120 (4), pp 833–838.

[7] D. Barik and M. Mondal, "Object identification for computer vision using image segmentation," 2010 2nd International Conference on Education Technology and Computer, Shanghai, China, 2010, pp. V2-170-V2-172, doi: 10.1109/ICETC.2010.5529412.

[8] F. Batzias, C. Siontorou, P.M. Spanidis, “Designing a reliable leak bio-detection system for natural gas pipelines” 2011. J. Hazard. Mater. 186, pp.35–58.

[9] F. Jalled, “Object Detection using Image Processing,” *Deep AI*, 23-Nov-2016. [Online]. Available: https://deepai.org/publication/object-detection-using-image-processing. [Accessed: 09-Mar-2021].

[10] G. L. FORESTI and S. GENTILI, “A VISION BASED SYSTEM FOR OBJECT DETECTION IN UNDERWATER IMAGES,” *International Journal of Pattern Recognition and Artificial Intelligence*, vol. 14, no. 02, pp. 167–188, 2000.

[11] G. S. Kumar, U. V. Painumgal, M. N. V. C. Kumar, and K. H. V. Rajesh, “Autonomous Underwater Vehicle for Vision Based Tracking,” *Procedia Computer Science*, vol. 133, pp. 169–180, 2018.

[12] H. Lu, T. Iseley, S. Behbahani, and L. Fu, “Leakage detection techniques for oil and gas pipelines: State-of-the-art,” *Tunnelling and Underground Space Technology*, 30-Jan-2020. [Online]. Available: https://www.sciencedirect.com/science/article/pii/S0886779818311131. [Accessed: 09-Mar-2021].

[13] “Image Feature Extraction using Hough Transformation Principle.” [Online]. Available: https://www.irjet.net/archives/V5/i3/IRJET-V5I3926.pdf. [Accessed: 09-Mar-2021].

[14] “Instantaneous Position and Orientation of the Body ...” [Online]. Available: http://www.scielo.org.mx/pdf/rmib/v35n3/v35n3a4.pdf. [Accessed: 09-Mar-2021].

[15] “Investigation of Vision-Based Underwater Object Detection ...” [Online]. Available: https://journals.sagepub.com/doi/pdf/10.5772/60526. [Accessed: 09-Mar-2021].

[16] J. Horgan, D. Toal, P. Ridao, and R. Garcia, “REAL-TIME VISION BASED AUV NAVIGATION SYSTEM USING A COMPLEMENTARY SENSOR SUITE,” *IFAC Proceedings Volumes*, 21-Apr-2016. [Online]. Available: https://www.sciencedirect.com/science/article/pii/S1474667015321248. [Accessed: 09-Mar-2021].

[17] J. Loth, G.J. Morris, G.M. Palmer, G.M., R. Guiler, D. Mehra, “Technology assessment of on-line acoustic monitoring for leaks/infringements in underground natural gas transmission lines”, 2003, West Virginia University, USA.

[18] J. Wang and Y. Su, "Underground object detection based on cross correlation and Hough transform," *2011 MICROWAVES, RADAR AND REMOTE SENSING SYMPOSIUM*, Kiev, Ukraine, 2011, pp. 363-366, doi: 10.1109/MRRS.2011.6053674.

[19] L. Shi *et al*., "An underwater pipeline tracking system for amphibious spherical robots," *2017 IEEE International Conference on Mechatronics and Automation (ICMA)*, Takamatsu, 2017, pp. 1390-1395, doi: 10.1109/ICMA.2017.8016020.

[20] M. A. Adegboye, A. Karnik, and W.-K. Fung, “Recent Advances in Pipelines Monitoring and Oil Leakage ...,” 04-Jun-2019. [Online]. Available: https://www.preprints.org/manuscript/201905.0041/v1/download. [Accessed: 09-Mar-2021].

[21] M. Kotani, M. Katsura, S. Ozawa, “Detection of gas leakage sound using modular neural networks for unknown environments”, 2004, Neurocomputing 62, pp 427–440.

[22] M. Narimani, S. Nazem and M. Loueipour, "Robotics vision-based system for an underwater pipeline and cable tracker," *OCEANS 2009-EUROPE*, Bremen, Germany, 2009, pp. 1-6, doi: 10.1109/OCEANSE.2009.5278327.

[23] O. A. Aguirre-Castro, E. Inzunza-González, E. E. García-Guerrero, E. Tlelo-Cuautle, O. R. López-Bonilla, J. E. Olguín-Tiznado, and J. R. Cárdenas-Valdez, "Design and Construction of an ROV for Underwater Exploration," *MDPI*, 06-Dec-2019. [Online]. Available: https://www.mdpi.com/1424-8220/19/24/5387/htm. [Accessed: 09-Mar-2021].

[24] P.S. Murvay, I. Silea, "A survey on gas leak detection and localization techniques",1992, J.Loss Prev. Process Ind. 25, pp 966–973

[25] R. Hussain, M. R. Juhari, N. W. Kang, R. C. Ismail, and A. Kamarudin, "Digital Image Processing Techniques for Object Detection From Complex Background Image," *Procedia Engineering*, 25-Aug-2012. [Online]. Available: https://www.sciencedirect.com/science/article/pii/S1877705812025684. [Accessed: 09-Mar-2021].

[26] R.K. Miller, "Acoustic emission leak detection", 1996, Final Report No. R96-472 to the New Jersey Institute of Technology.

[27] S. Ahmed, M. F. R. Khan, M. F. A. Labib and A. E. Chowdhury, "An Observation of Vision Based Underwater Object Detection and Tracking," *2020 3rd International Conference on Emerging Technologies in Computer Engineering: Machine Learning and Internet of Things (ICETCE)*, Jaipur, India, 2020, pp. 117-122, doi: 10.1109/ICETCE48199.2020.9091752

[28] S. Guiming and S. Jidong, "Remote sensing image edge-detection based on improved Canny operator," *2016 8th IEEE International Conference on Communication Software and Networks (ICCSN)*, Beijing, China, 2016, pp. 652-656, doi: 10.1109/ICCSN.2016.7586604

[29] S.M. Folga, "Natural gas pipeline technology overview", 2007, Tech. Rep. Argonne National Laboratory..

[30] S. Sadovnychiy, I. Bulgakov, and J. Valadez, "System for Remote Detection of Pipeline Leakage," *OnePetro*, 20-Jun-2005. [Online]. Available: https://onepetro.org/SPELACP/proceedings/05LACPEC/All-05LACPEC/SPE-94958-MS/73004. [Accessed: 09-Mar-2021]. .

[31] S. Scott, M. Barrufet, "Worldwide assessment of industry leak detection capabilities for single & multiphase pipelines", 2003, Tech. rep. Dept. of Petroleum Engineering. A&M University, Texas.

[32] Tang, Xiujia, Yan, Dachun, "Pipeline leak detection method and instrument based on neural networks", 1997, At ca Scientiarum Naturalium Universitis Pekinensis 33, pp 319–327.

[33] V. Antipov, V. Kokovkina, V. Kirnos and A. Priorov, "Computer vision system for recognition and detection of color patterns in real-time task of robot control," 2017 *Systems of Signal Synchronization, Generating and Processing in Telecommunications* (SINKHROINFO), Kazan, 2017, pp. 1-5, doi: 10.1109/SINKHROINFO.2017.7997496.

[34] V. N. Dobrokhodov, I. I. Kaminer, K. D. Jones and R. Ghabcheloo, "Vision-based tracking and motion estimation for moving targets using small UAVs," *2006 American Control Conference*, Minneapolis, MN, USA, 2006, pp. 6 pp.-, doi: 10.1109/ACC.2006.1656418.

[35] "Vision-based system of AUV for an underwater pipeline tracker." [Online]. Available: https://www.researchgate.net/publication/257802439_Vision-based_system_of_AUV_for_an_underwater_pipeline_tracker. [Accessed: 09-Mar-2021].

[36] W. Qing-shu, T. Yu-fei and Z. Jin-hui, "Analysis of Influence of Leakage in a Branch Pipeline on Pipeline Network Running Characteristics," *2010 Third International Conference on Information and Computing*, Wuxi, China, 2010, pp. 190-193, doi: 10.1109/ICIC.2010.232.

[37] X. Zhao, L. Jing and Z. Du, "Research on Image Segmentation Method of Underwater Pipeline Oil Leakage Point," 2020 IEEE International Conference on Mechatronics and Automation (ICMA), Beijing, China, 2020, pp. 165-170, doi: 10.1109/ICMA49215.2020.9233698.

[38] Y. Li, L. Sun, L. K. Wang and L. L. Zhang, "Design of leakage detection and location system for long range crude oil pipeline," *IEEE ICCA 2010*, Xiamen, China, 2010, pp. 1742-1746, doi: 10.1109/ICCA.2010.5524309.

[39] Y. Deng and H. Wang, "Underwater Circular Object Positioning System Based on Monocular Vision," *2019 IEEE International Symposium on Signal Processing and Information Technology (ISSPIT)*, 2019.

[40] Z. Chen, Z. Zhang, F. Dai, Y. Bu, and H. Wang, "Monocular Vision-Based Underwater Object Detection," 24-May-2017. [Online]. Available: https://pdfs.semanticscholar.org/d32b/8bf20b50e79e5a16dd18cadbd3a8a1177ace.pdf. [Accessed: 09-Mar-2021].

VITA AUCTORIS

NAME: Manisha Alkarim Thobhani

PLACE OF BIRTH: India

YEAR OF BIRTH: 1982

EDUCATION: Bachelor of Electrical Engineering, Saurashtra University, India, 2005.

Master of Applied Science in Industrial Engineering, University of Windsor, Windsor, Ontario, Canada, 2020

.